19

AFCRL-66-812

ATMOSPHERIC ABSORPTIONS OVER LONG SLANT PATHS IN THE STRATOSPHERE

David G. Murcray, Frank H. Murcray
and
Walter J. Williams

Department of Physics
University of Denver
Denver, Colorado

Contract AF 19(628)-5202

Project 8662

Task 866201

Scientific Report No. 4

October 1966

This research was sponsored by the Advanced Research Projects Agency under ARPA Order No. 363

Prepared for

Air Force Cambridge Research Laboratories
Office of Aerospace Research
United States Air Force
Bedford, Massachusetts

AFCRL-66-812

ATMOSPHERIC ABSORPTIONS OVER LONG SLANT PATHS IN THE STRATOSPHERE

David G. Murcray, Frank H. Murcray
and
Walter J. Williams

Department of Physics
University of Denver
Denver, Colorado

Contract AF 19(628)-520

Project 8662

Task 866201

Scientific Report No. 4

October 1966

This research was sponsored by the Advanced Research Projects Agency
under ARPA Order No. 363

Prepared for

Air Force Cambridge Research Laboratories
Office of Aerospace Research
United States Air Force
Bedford, Massachusetts

BLANK PAGE

TABLE OF CONTENTS

		Page
	ABSTRACT	vi
1.	INTRODUCTION	1
2.	INSTRUMENTATION	2
3.	FLIGHT DETAILS	3
4.	RESULTS	4
5.	DISCUSSION	5
6.	ACKNOWLEDGMENTS	10
7.	REFERENCES	11

LIST OF FIGURES

Figure No.		Page
1	Atmospheric transmittance versus wavenumber as observed at various altitudes for the region 3890-3740 cm^{-1}, Rec. 12-53	12
2	Atmospheric transmittance versus wavenumber as observed at various altitudes for the region 3920-3790 cm^{-1}, Rec. 31-39	14
3	Atmospheric transmittance versus wavenumber as observed at various altitudes for the region 3800-3670 cm^{-1}, Rec. 31-39	16
4	Atmospheric transmittance versus wavenumber as observed at various altitudes for the region 3680-3540 cm^{-1}, Rec. 31-39	18
5	Atmospheric transmittance versus wavenumber as observed at various altitudes for the region 3920-3790 cm^{-1}, Rec. 46-51	20
6	Atmospheric transmittance versus wavenumber as observed at various altitudes for the region 3800-3670 cm^{-1}, Rec. 46-51	22
7	Atmospheric transmittance versus wavenumber as observed at various altitudes for the region 3690-3560 cm^{-1}, Rec. 46-51	24
8	Atmospheric transmittance versus wavenumber as observed at various altitudes for the region 3920-3790 cm^{-1}, Rec. 54-70	26
9	Atmospheric transmittance versus wavenumber as observed at various altitudes for the region 3800-3670 cm^{-1}, Rec. 54-70	28
10	Atmospheric transmittance versus wavenumber as observed at various altitudes for the region 3680-3540 cm^{-1}, Rec. 54-70	30
11	Atmospheric transmittance versus wavenumber as observed at various altitudes for the region 3920-3790 cm^{-1}, Rec. 12-18	32

LIST OF FIGURES (Cont.)

Figure No.		Page
12	Atmospheric transmittance versus wavenumber as observed at various altitudes for the region 3800-3670 cm^{-1}, Rec. 12-18	34
13	Atmospheric transmittance versus wavenumber as observed at various altitudes for the region 3680-3550 cm^{-1}, Rec. 12-18	36
14	Atmospheric transmittance versus wavenumber as observed at various altitudes for the region 3920-3790 cm^{-1}, Rec. 19-28	38
15	Atmospheric transmittance versus wavenumber as observed at various altitudes for the region 3800-3670 cm^{-1}, Rec. 19-28	40
16	Atmospheric transmittance versus wavenumber as observed at various altitudes for the region 3690-3560 cm^{-1}, Rec. 19-28	42
17	Atmospheric transmittance versus wavenumber as observed at various altitudes for the region 3920-3790 cm^{-1}, Rec. 37-43	44
18	Atmospheric transmittance versus wavenumber as observed at various altitudes for the region 3800-3690 cm^{-1}, Rec. 37-43	46
19	Comparison of the transmittance observed with the transmittance predicted by Plass[4] in the 3800 cm^{-1} to 3730 cm^{-1} region	48
20	Comparison of the transmittance observed with the transmittance predicted by Plass[4] in the 3800 cm^{-1} to 3730 cm^{-1} region	48
21	Water vapor mixing ratio profile as determined from the variation of the infrared absorption with altitude	49

ABSTRACT

The variation of the infrared solar spectrum with altitude was observed during a series of balloon flights made from Fairbanks, Alaska. Spectra were obtained at various altitudes with solar zenith angles ranging from 49° to 92°. These spectra were used to determine the atmospheric transmittance to be expected at high altitudes and particularly over very long slant paths in the stratosphere. The transmittance data are presented in this report.

The spectral region scanned during these flights covered the 2.7μ region. The major atmospheric absorptions in this region are due to carbon dioxide and water vapor. The paths traversed by the solar radiation in reaching the spectrometer when the solar zenith angle is greater than 90° are such that a major portion of the air mass traversed by the radiation is traversed in a relatively narrow altitude interval close to the minimum height of the ray. Thus these long paths provide a method of sampling the absorption to be expected in relatively narrow layers. The water vapor absorptions obtained under these conditions have been used to determine the amount of water vapor present in these layers in the stratosphere. These data are compared with the mixing ratios determined on the basis of the change in these absorptions during a flight with small solar zenith angle. The agreement is within the accuracy of the measurement and shows no indication that the data of the normal flight are inaccurate due to contamination. The profile indicates the increased mixing ratio above the tropopause noted on other flights at other geographic locations.

1. INTRODUCTION

In previous reports[1, 2] we have presented data showing the spectral transmittance of the earth's atmosphere at high altitudes. These data have been obtained during a series of balloon flights made with a balloon-borne spectrometer system flown in conjunction with a biaxial pointing control which orients a telescope such that the solar image is formed on the spectrometer entrance slit. Due to the problems associated with flying balloons, these flights are launched close to sunrise and the flights terminated before sunset in order to implement recovery of the equipment. Thus most of the spectra are obtained with the sun high in the sky and the optical air mass traversed by the solar radiation at high altitudes is small. In order to obtain data pertinent to the transmittance over long slant paths at high altitudes, using the sun as a source, it is necessary to obtain data with the sun low in the sky, i.e., sunrise or sunset. The period during which such data can be obtained is limited at the lower latitudes; however, in the high Northern latitudes during June and July the sun never sets at balloon altitudes and there is a period of several hours when spectra can be obtained with solar zenith angles of 90° or more. In order to obtain transmittance data over such paths, and also to obtain data at geographic locations other than the normal mid-latitude sites, a series of balloon flights was made from Fairbanks, Alaska, during the summer of 1964. The data obtained during these flights are presented in this report.

2. INSTRUMENTATION

The balloon-borne instrumentation employed in obtaining the data presented in this report consisted of the following basic units: A Czerny-Turner 1/2 meter grating spectrometer, a biaxial pointing control or "sun seeker," an on-board digital magnetic tape recorder, an on-board FM-analog magnetic tape recorder, an FM/FM telemetry system, power supplies for operating the various units, a balloon command package, and a gondola in which the units are mounted and which protects the equipment when it is returned to the ground via parachute. The units are described in detail in an article to be published in the February 1967 issue of Applied Optics.[3]

For these flights two magnetic tape recording systems were used for on-board recording. The primary system was a digital system described in the referenced article. Since this unit was being used for the first time, the analog FM recorder used on previous flights was flown as backup. This unit is a 4-channel unit, also designed and constructed by project personnel for balloon use.

The rectified detector output voltage was recorded in 4 channels of the digital recorder and on one channel of the FM recorder. The ac signal from the detector was also recorded on one channel of the FM recorder. The other channels were used to record auxiliary data pertinent to the experiment and to monitor the performance of various units.

The balloon instrumentation used in this study represented a considerable investment in time and money, hence recovery of the instrumentation was essential. Since upper wind information is generally sparse and balloon ascent rates quite often differ from predicted, it is very difficult to predict accurately where the balloon will be with respect to the ground at any particular time. It is quite often necessary, therefore, to change flight plans as the flight trajectory develops. A real time readout of the performance of the instrumentation is of great value in making such decisions. An FM/FM telemetry system was also included as part of the balloon instrumentation to provide this real time information. It was also used as a further backup recording of the primary data. The airborne system consisted of 4 standard IRIG voltage-controlled sub-carrier oscillators which fed a 4 watt FM transmitter operated at 249.9 megacycles. The data from this system was recorded on the ground in multiplex form on magnetic tape. In addition one channel of the multiplexed signal was also fed to a discriminator

and the output of the discriminator was recorded using a visicorder. The channel monitored in this fashion had the ac signal from the spectrometer as its input. This channel was chosen since it provided an excellent evaluation of the overall system performance.

3. FLIGHT DETAILS

3.1 Balloon Flight of July 7-8 (A1)

The first flight of this series was launched at 2120 AST July 7, 1964, after a two hour delay due to surface winds. At the time the balloon was launched the sun had set on the ground. The balloon ascended with an average ascent rate of 150 m/min and reached a floating altitude of 29 km at 0035 AST July 8. The balloon was allowed to float until 0436 AST. The equipment impacted at 151°41' W longitude, 65°01' N latitude, and was recovered by helicopter.

3.2 Balloon Flight of July 13-14 (A2)

After renovation the equipment was launched the second time at 1904 AST July 13 and ascended with an average ascent rate of 200 m/min until the balloon reached approximately 10 km. At this time the ascent rate started decreasing and at an altitude of 13 km the balloon had stopped ascending. Ballast was released by radio command, but the ascent rate achieved during the remainder of the flight was less than 100 m/min. The flight was terminated at 0210 AST July 14. The equipment impacted at 149°29' W longitude, 64°11' N latitude. Recovery was accomplished by helicopter.

3.3 Balloon Flight of July 21 (A3)

The final flight of the series was launched at 1352 AST July 21, 1964. The balloon ascent rate was normal and an overall ascent rate of 200 m/min was achieved. The balloon reached a floating altitude of 31 km. The flight was terminated at 1803 AST to facilitate recovery. The equipment impacted at 147°31' W longitude, 64°39' N latitude, and was recovered using a helicopter. Impact on all flights was soft and no damage was incurred due to impact.

4. RESULTS

The digital magnetic data tapes were played back into a computer, and selected spectra from each flight were plotted. Examination of these spectra revealed that they all contained many false absorptions that were not present in the ac data. It was determined that these were the result of momentary loss of synchronization in the synchronous rectification system, caused by the tines of the tuning fork chopper bumping together. This bumping occurred at altitudes in excess of 20,000 feet and was due to the fact that the oscillation was air damped. As the air density decreased the amplitude increased until at altitudes above 20,000 feet the tines started bumping. While this affected the synchronous rectification the ac data were not affected. In view of this the ac data were used in the data reduction.

Although the analog spectra as recorded contain considerable information, it is necessary, for purposes of quantitative analysis, to convert the data to % transmittance versus wavelength. In order to do this it is necessary to determine what the voltage from the detector would have been if the absorption were not present, i.e., the so-called vacuum envelope. This is generally determined on the basis of the spectra recorded at altitude when the absorptions are minimal. On the first flight of this series the overall signal level from the infrared detector was significantly less than on the other two flights. This appears to have been due to the scattering of the solar radiation in traversing the long slant path in the atmosphere. While this relatively non-selective attenuation is of interest the primary concern of this study was with the selective absorption. In view of this the vacuum envelope was determined on the basis of signal recorded in the window regions between groups of absorption lines. Thus the data represent the attenuation due to molecular absorption, and does not include that due to scattering. Once the envelopes had been determined the analog records were digitized and the percent transmission was determined as a function of wavenumber using a digital computer. Selected plots of the spectral transmittance versus wavenumber, as observed under various conditions during the three flights, are given in Figures 1 through 18.

5. DISCUSSION

As mentioned above the purpose of these flights was to gather data concerning the attenuation of infrared radiation in traversing long slant paths in the earth's atmosphere. The type of path traversed by the radiation when the sun is low in the sky is illustrated below. For obvious reasons the drawing is not to scale.

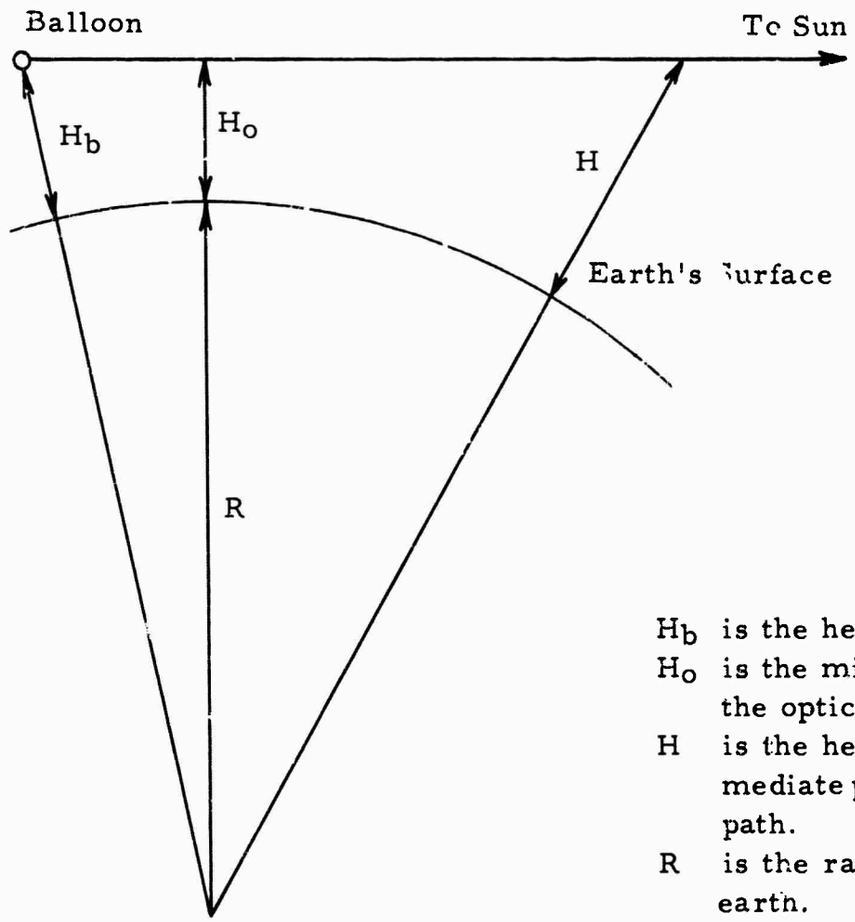

H_b is the height of balloon.
H_o is the minimum height of the optical path.
H is the height of an intermediate point on the optical path.
R is the radius of the earth.

Since the plane parallel atmosphere approximation is not valid in this case it is necessary to trace the ray through the atmosphere and calculate $\int_H^\infty \rho(h)\,dh$ along the ray in order to determine the amount of absorbing material traversed by the radiation. In performing the ray tracing calculations refraction effects must be taken into account; however, in the cases where the path lies wholly in the stratosphere,

the effects of refraction are small and for purposes of the following discussion can be neglected. Neglecting refraction the length of the path L from H_o to an arbitrary point a distance H above the earth's surface is given by

$$L = \sqrt{(R+H)^2 - (R+H_o)^2} = \sqrt{2RH+H^2 - 2H_oR-H_o^2}$$

$$L = \sqrt{[2(R+H_o) + H-H_o][(H-H_o)]}$$

or neglecting $H-H_o$ with respect to $2(R+H_o)$ one has

$$L = \sqrt{2(R+H_o)(H-H_o)}$$

If one splits the atmosphere into layers, the length ℓ, in the layer is given by

$$\ell = \sqrt{2(R+H_o)}\left[\sqrt{(H_{i+1}-H_o)} - \sqrt{H_i - H_o}\right]$$

and the mass of air traversed by the radiation can be determined from

$$m = \sum_i \sqrt{2(R+H_o)}\left\{\sqrt{H_{i+1}-H_o} - \sqrt{H_i - H_o}\right\}\overline{\rho}_i$$

where $\overline{\rho}_i$ is the average density in the i^{th} layer, and the summation is performed over the layers from the balloon down to the minimum height H_o and then from H_o out to the point where the density has fallen off to where any further contribution can be neglected. It one calculates the air mass traversed in a typical path of this type for balloon altitudes, the air mass traversed by the radiation from balloon altitude down to minimum altitude H_o and back to balloon altitude is quite often considerably more than half of the total air mass traversed by the radiation. The pressure at balloon altitude is sufficiently large that over the lower part of the path the Lorentz line shape predominates. In this case the absorption depends on the $\int P\,dw$ along the path. The inclusion of the pressure weights the lower altitude layers so that this dependence of the absorption on the lower layers is further enhanced. Thus this type of path provides an excellent method of studying the variation with altitude of the absorbing constituents. The extent of this affect in the spectra obtained during the first and second flights is evident in the data given in Table I. In this table the air mass traversed by the radiation in that portion of the path from the balloon down to the minimum altitude and back up to the balloon altitude is given, along

with the total air mass traversed by the radiation. Once the solar zenith angle becomes much greater than 90° the air mass traversed in this layer becomes more than half of the total air mass.

The solar spectra obtained during the first two flights of this series indicate the transmittance to be expected in this wavelength region over long slant paths in the stratosphere. If one compares these spectra with solar spectra taken at lower altitude but high sun, one finds greater transmittance at the higher altitudes, even though the air masses traversed during these flights are considerably greater (approximately 8 air masses in the case of record 37 on the July 7, flight compared with 1.5 air masses in a normal ground record). The increase in transmittance at the higher altitude is the result of two factors. First, the absorptions in this spectral region are pressure dependent, and the reduced atmospheric pressure at the higher altitudes reduces the absorption due to equivalent amounts of absorbing material. Second, the amount of water vapor present per unit air mass is considerably less at the higher altitudes. Thus the observed transmittances are in quantitative agreement with what one would predict on a theoretical basis.

All evidence currently available indicates that carbon dioxide is uniformly distributed in the earth's atmosphere. Assuming that this is the case, and that its abundance is ~0.03% by volume, it is possible to compare the transmittance observed over these long stratospheric paths with the transmittances predicted by Plass.[4] Previous comparisons between his predicted transmittances and our observed transmittances had indicated relatively good agreement for carbon dioxide absorptions. The major carbon dioxide absorptions in this region are due to the two bands centered at 3716 cm^{-1} and 3609 cm^{-1}. The transmittances in the vicinity of the 3716 cm^{-1} band observed during the flight made July 7, (spectrum number 37) are compared with those given by Plass for 2000 atm-cm of CO_2 at a temperature of 200°K and pressures of 0.1 atm and 0.2 atm in Figure 19. As pointed out above, the major portion of the absorption in this type of path occurs in the layer between the balloon and the minimum height of the ray Thus for record 37 the radiation had traversed approximately 2000 atm-cm of CO_2, the majority of which is at a pressure of approximately .07 atm. At first sight it would appear that the theoretical transmittance curve does not fall off as rapidly as it should as one approaches the band center; however, it should be remembered that the theoretical curves are for CO_2 absorption only, while the experimental are the result of absorptions by CO_2 and H_2O. H_2O has a group of strong lines in the vicinity of 3750 cm^{-1}. The absorptions in the region from 3800 to 3760 cm^{-1} are also due to H_2O.

Figure 20 shows a similar comparison for spectrum number 53. In this case the radiation had traversed approximately 750 atm-cm of CO_2, the majority of which was at a pressure of 0.03 atm. If one makes allowance for the fact that the observed absorptions are due to H_2O as well as CO_2, the agreement between the theoretical predictions and the observations is satisfactory.

Water vapor absorptions occur throughout the region scanned during these flights. The absorptions occurring between 3791 cm^{-1} and 3860 cm^{-1}, in particular, are due mainly to a series of strong water vapor lines. The distribution of water vapor above 13 km is currently the subject of controversy. The opinions concerning the distribution range from the view that the water vapor is uniformly mixed above the tropopause with a constant relatively "dry" mixing ratio of $2 \cdot 10^{-6}$ g/g to the view that the mixing ratio above the tropopause is variable and often relatively wet, i.e., mixing ratios of approximately 10^{-4} g/g at various altitudes. The water vapor absorptions observed during the various balloon flights made previously have been characterized by a very rapid fall-off in absorption as the balloon approaches the tropopause followed by a very slow decrease in absorption above the tropopause and a significant residual absorption at altitude. Using these absorptions to determine a water vapor mixing ratio profile, one obtains a profile which decreases to a low value ($\sim 2 \cdot 10^{-6}$ g/g) in the lower stratosphere with an increase in the mixing ratio above 20 km, and an average mixing ratio above the balloon of between 10^{-5} g/g and 10^{-4} g/g. The results of these measurements have been questioned on the basis that if the balloon or the instrumentation is outgassing water vapor, then part of the measured mixing ratio would be due to contamination. The solar spectra obtained during the first two flights are characterized by the fact that the radiation has traversed long paths in the stratosphere and relatively large air masses. As a result, any contamination which might be present becomes insignificant in comparison with the absorptions due to the atmospheric water vapor. Houghton and Seeley[5] give a series of curves of growth for the water vapor absorptions in the region from 3791 cm^{-1} to 3860 cm^{-1}. These curves relate $\sqrt{uP/P_o}$ with the integrated absorption over the region from 3791 - 3811 cm^{-1}, 3811 - 3830 cm^{-1}, 3830 - 3847 cm^{-1}, and 3847 - 3860 cm^{-1}. The integrated absorptions over these regions were determined for the various spectra obtained during the first two flights and the absorptions were used to determine the values for $\sqrt{uP/P_o}$. The values of $\sqrt{uP/P_o}$ determined for each spectrum were compared. If the values were in good agreement the values were averaged, and the average value was used to determine the amount of water vapor and the mixing ratio. This quantity is really the integral of the water

vapor content times the pressure over the total path. Since the water vapor distribution is not known this integral cannot be determined. It has been pointed out above that the major portion of the optical path occurs in the layer between the balloon and the minimum point along the path. In determining the mixing ratio the assumption was made that the water vapor is all concentrated in this layer. This has the effect of reducing the overall amount of water vapor required to account for the observed absorptions by placing it all in the higher pressure environment. In determining mixing ratio the total air mass traversed by the radiation was assumed to be concentrated in this layer. Thus all mixing ratios determined from these spectra are too "dry", i.e., they are biased toward low mixing ratios. The mixing ratios determined in this fashion are given in Table II. Unfortunately, because of the low ascent rates achieved during these flights, no data were obtained where the minimum altitude along the path was higher than 21.6 km, and the average height of the layer was about 22-23 km.

The third flight of the series was launched when the sun was relatively high in the sky and the solar zenith angles encountered during the flight were characteristic of those encountered during flights made at low latitude launch sites. During this type of flight the absorptions decrease as the balloon ascends, and it is possible to determine a water vapor mixing ratio profile on the basis of the change in absorption with altitude. A profile was determined on the basis of the variation with altitude of the region from 3847 - 3860 cm^{-1}. The profile determined in this fashion is given in Figure 21. Comparison of the results with those determined from the long path absorptions indicates that they agree reasonably well, and the mixing ratio profile determined on the basis of a normal daytime ascent is not significantly contaminated. In comparing the results, one must keep in mind the uncertainties in the curves of growth of the absorptions and in the air mass traversed by the radiation in the long path case. Thus the long path data confirm the fact that the mixing ratio increases at altitudes in excess of 20 kms.

ACKNOWLEDGEMENTS

The authors want to express their appreciation for the excellent support received from the Air Force Cambridge Research Laboratories Balloon Group who performed the launch of the balloons and the recovery of the instrumentation on these flights, and to the U. S. Army Arctic Test Center for their support of the operation. Our thanks also to Jim Brooks, Warren Cochran, John Kosters and Steve Smith for their assistance in performing the flight and to Charles Garwood and Marie Working for assisting in the data reduction.

REFERENCES

1. Murcray, D. G., F. H. Murcray and W. J. Williams, Scientific Report No. 1, Contract AF 19(628)-5202.

2. Murcray, D. G., F. H. Murcray and W. J. Williams, Scientific Report No. 3, Contract AF 19(628)-5202.

3. Murcray, D. G., F. H. Murcray and W. J. Williams, "A Balloon Borne Grating Spectrometer," to be published in Applied Optics, February 1967.

4. Plass, G. N., V. R. Stull and P. J. Wyatt, Final Report, Vol. III, Contract AF 04(695)-96.

5. Houghton, J. T. and J. S. Seeley, Quarterly Journal of the Royal Meteorological Society 86, p. 358 (1960).

Figure 1

Atmospheric transmittance versus wavenumber as observed at various altitudes for the region 3890-3740 cm^{-1}.

Fairbanks, Alaska July 7, 1964

Rec.	Time (AST)	h (km)	P (mb)	Zenith $\measuredangle$
12	2214	11.3	215	90.39
23	2244	15.2	117	91.40
37	2327	20.4	52.2	92.23
53	0015	26.8	19.4	92.30

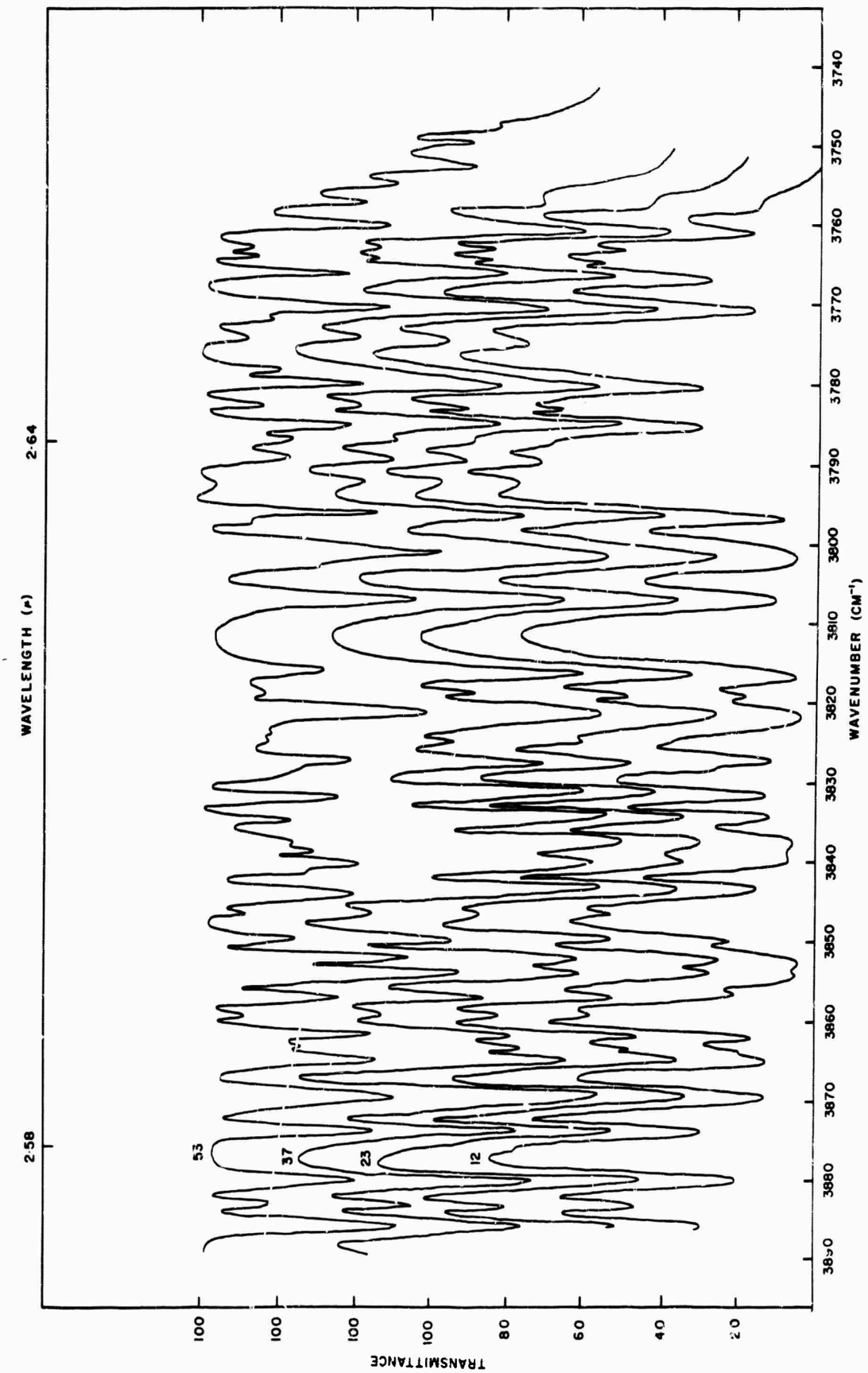
WAVELENGTH (μ)
2·58
2·64
WAVENUMBER (CM⁻¹)
3740
3750
3760
3770
3780
3790
3800
3810
3820
3830
3840
3850
3860
3870
3880
3890
TRANSMITTANCE
100
100
100
80
60
40
20
53
37
23
12

Figure 2

Atmospheric transmittance versus wavenumber as observed at various altitudes for the region 3920-3790 cm^{-1}.

Fairbanks, Alaska July 13, 1964

Rec.	Time (AST)	h (km)	P (mb)	Zenith $\measuredangle$
31	2048	14.3	136.5	86.67
32	2051	14.4	132.5	86.98
34	2057	15.0	121.5	87.40
36	2103	15.4	113.5	87.82
39	2112	16.7	93.0	88.42

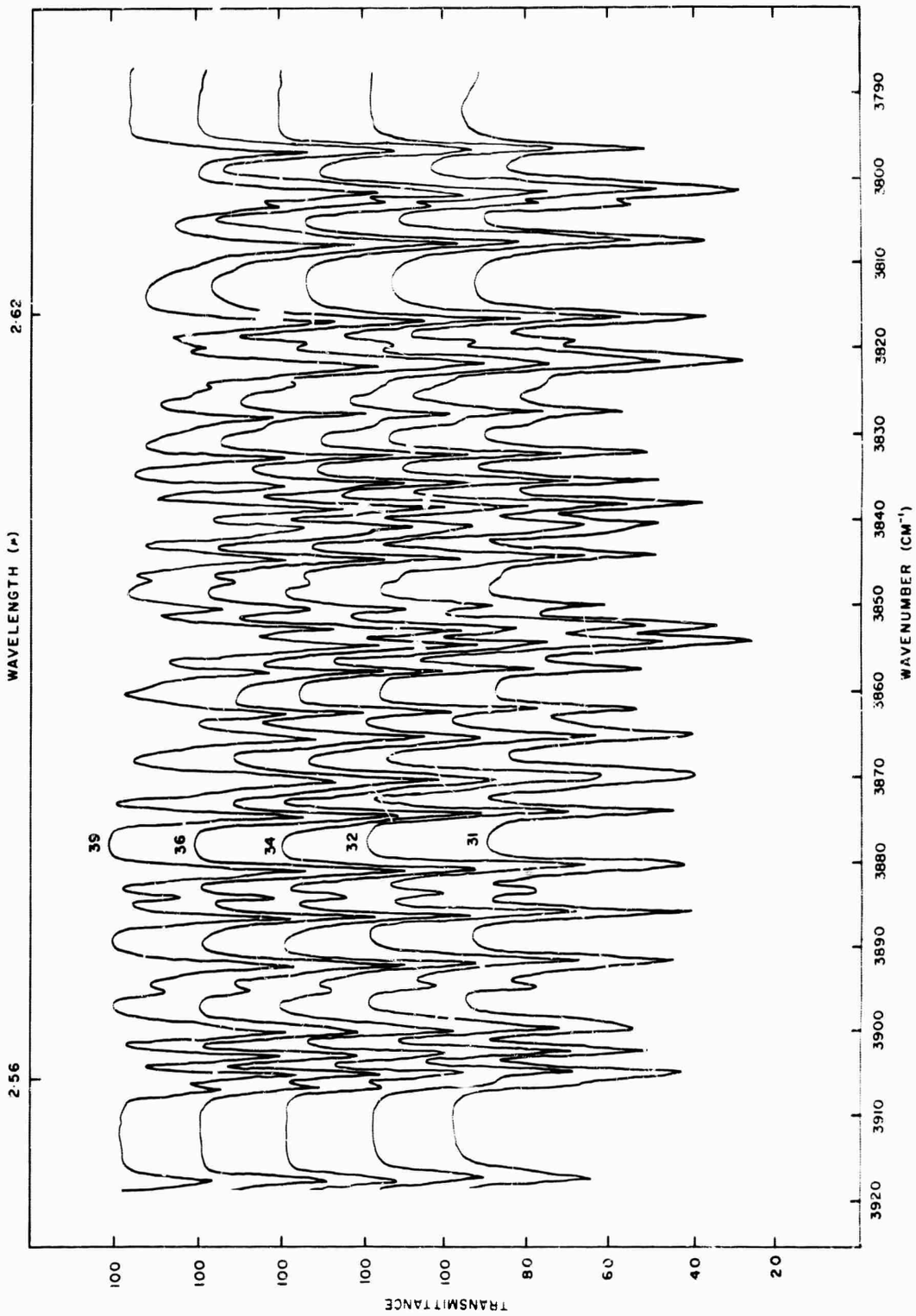
WAVELENGTH (μ)
2·56
2·62
WAVENUMBER (CM⁻¹)
3920
3910
3900
3890
3880
3870
3860
3850
3840
3830
3820
3810
3800
3790
TRANSMITTANCE
100
100
100
100
100
80
60
40
20
39
36
34
32
31

Figure 3

Atmospheric transmittance versus wavenumber as observed at various altitudes for the region 3800-3670 cm^{-1}.

Fairbanks, Alaska July 13, 1964

Rec.	Time (AST)	n (km)	P (mb)	Zenith ∢
31	2048	14.3	136.5	86.67
32	2051	14.4	132.5	86.98
34	2057	15.0	121.5	87.40
36	2103	15.4	113.5	87.82
39	2112	16.7	93.0	88.42

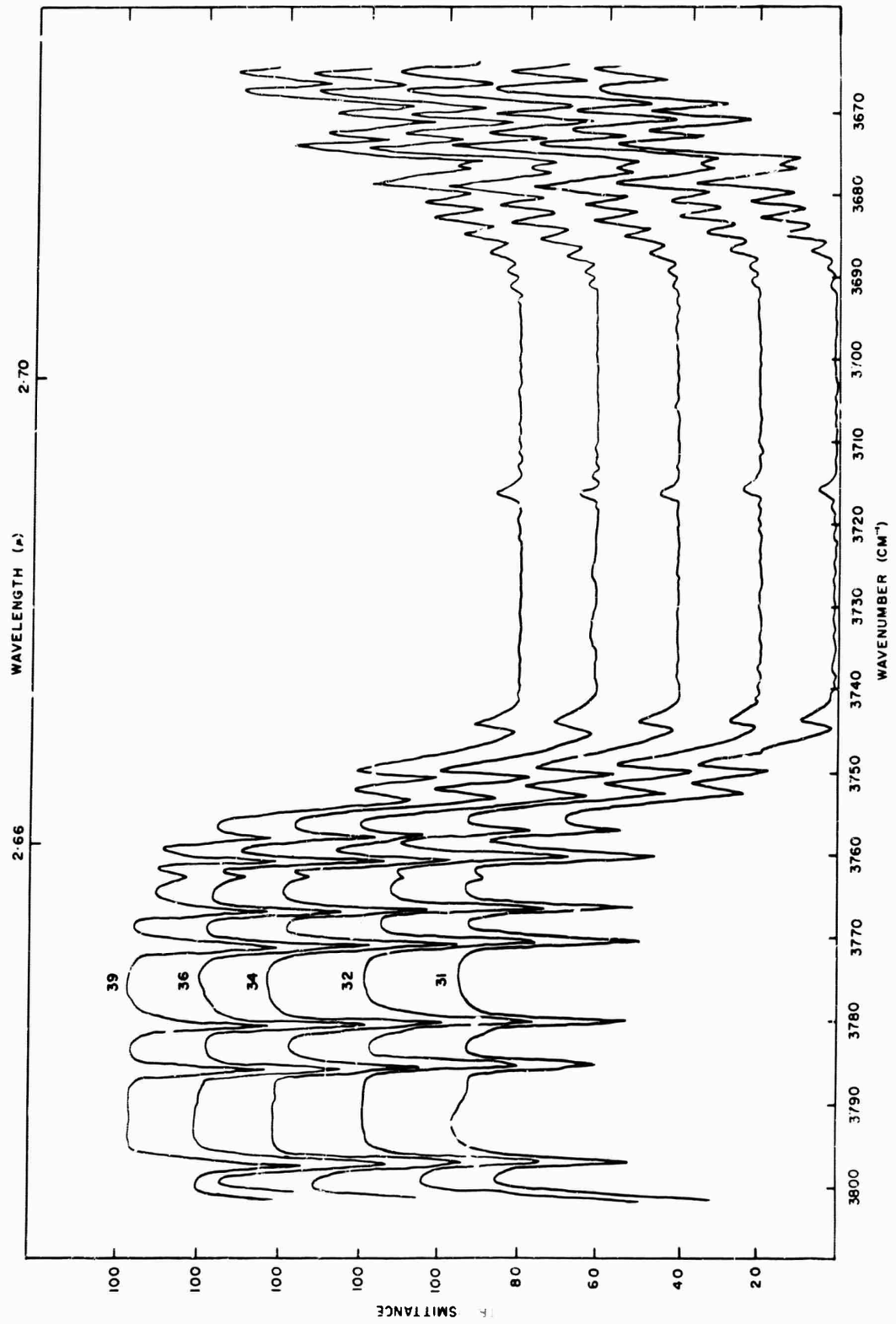
WAVELENGTH (μ)
2·66
2·70
WAVENUMBER (CM⁻¹)
3800
3790
3780
3770
3760
3750
3740
3730
3720
3710
3700
3690
3680
3670
TRANSMITTANCE
100
100
100
100
100
80
60
40
20
39
36
34
32
31

Figure 4

Atmospheric transmittance versus wavenumber as observed at various altitudes for the region 3680-3540 cm^{-1}.

Fairbanks, Alaska July 13, 1964

Rec.	Time (AST)	h (km)	P (mb)	Zenith ∢
31	2048	14.3	136.5	86.67
32	2051	14.4	132.5	86.98
34	2057	15.0	121.5	87.40
36	2103	15.4	113.5	87.82
39	2112	16.7	93.0	88.42

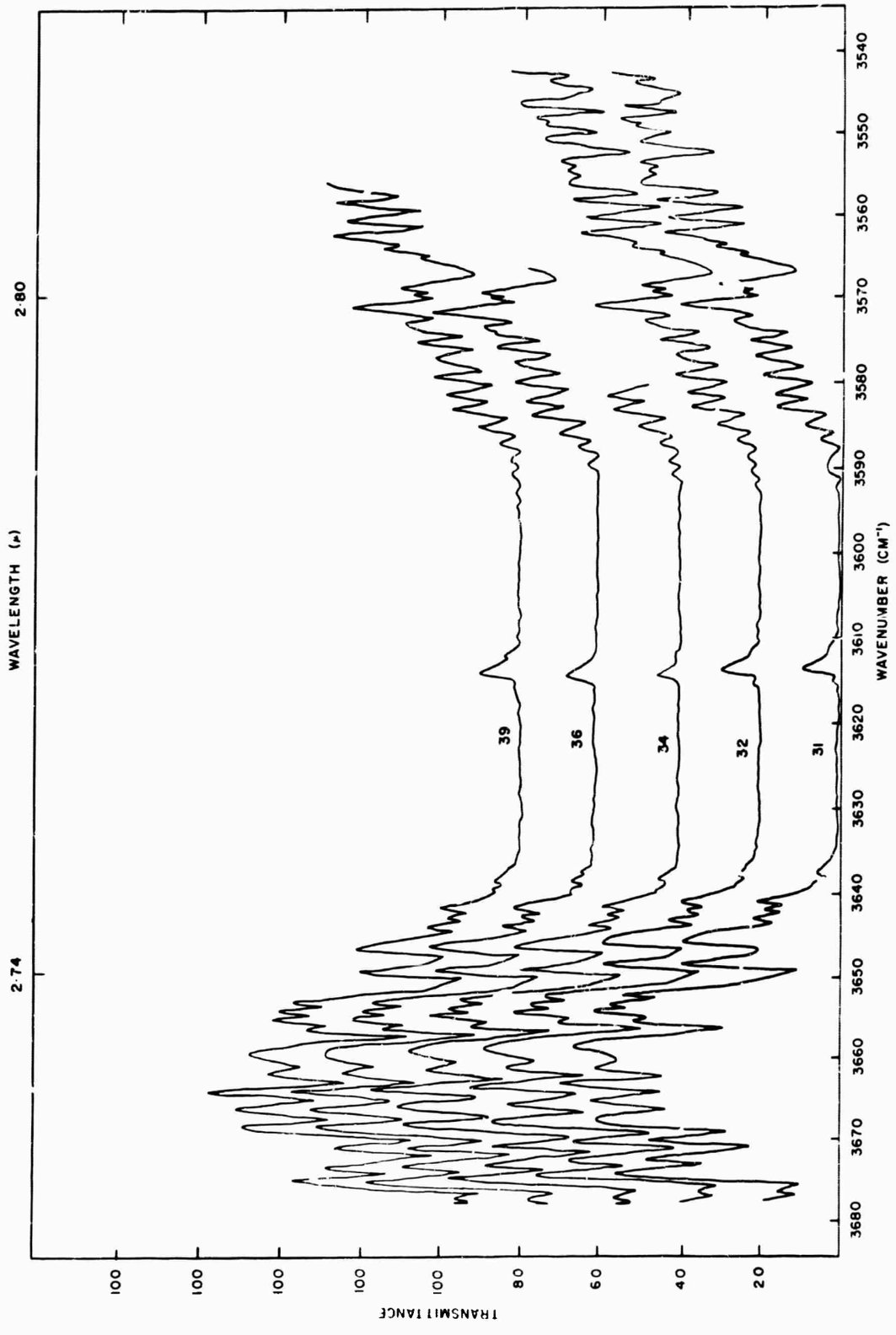
WAVELENGTH (μ)
2·74
2·80
WAVENUMBER (CM⁻¹)
3680
3670
3660
3650
3640
3630
3620
3610
3600
3590
3580
3570
3560
3550
3540
TRANSMITTANCE
100
100
100
100
80
60
40
20
39
36
34
32
31

Figure 5

Atmospheric transmittance versus wavenumber as observed at various altitudes for the region 3920-3790 cm^{-1}.

Fairbanks, Alaska July 13, 1964

Rec.	Time (AST)	h (km)	P (mb)	Zenith ∢
46	2133	19.2	62.7	89.74
49	2142	20.6	50.6	90.24
50	2145	21.0	47.7	90.40
51	2148	21.4	44.7	90.56

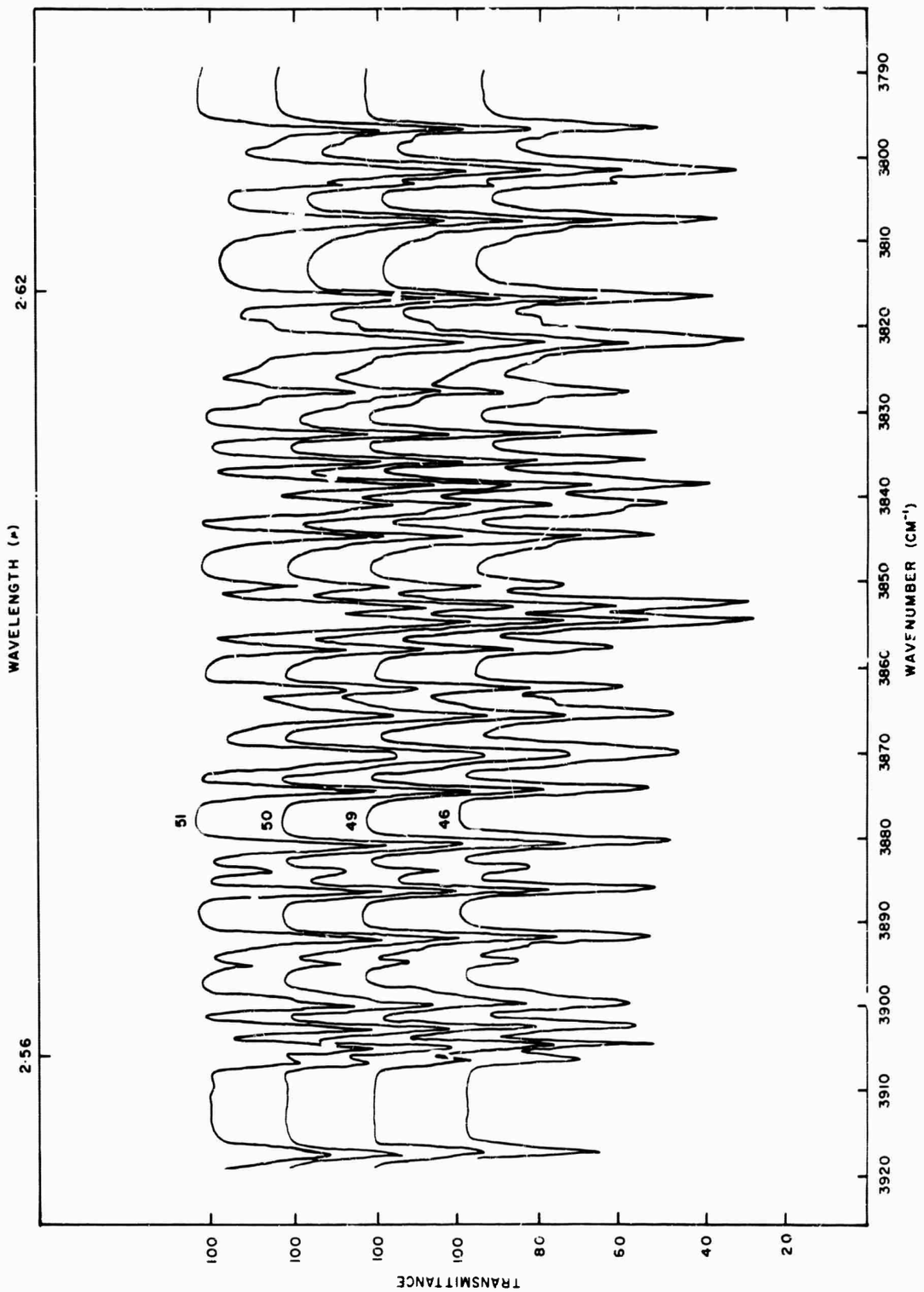
WAVELENGTH (μ)
2·56
2·62
WAVENUMBER (CM⁻¹)
3920
3910
3900
3890
3880
3870
3860
3850
3840
3830
3820
3810
3800
3790
TRANSMITTANCE
100
100
100
100
80
60
40
20
51
50
49
46

Figure 6

Atmospheric transmittance versus wavenumber as observed at various altitudes for the region 3800-3670 cm^{-1} .

Fairbanks, Alaska July 13, 1964

Rec.	Time (AST)	h (km)	P (mb)	Zenith ϕ
46	2133	19.2	62.7	89.74
49	2142	20.6	50.6	90.24
50	2145	21.0	47.7	90.40
51	2148	21.4	44.7	90.56

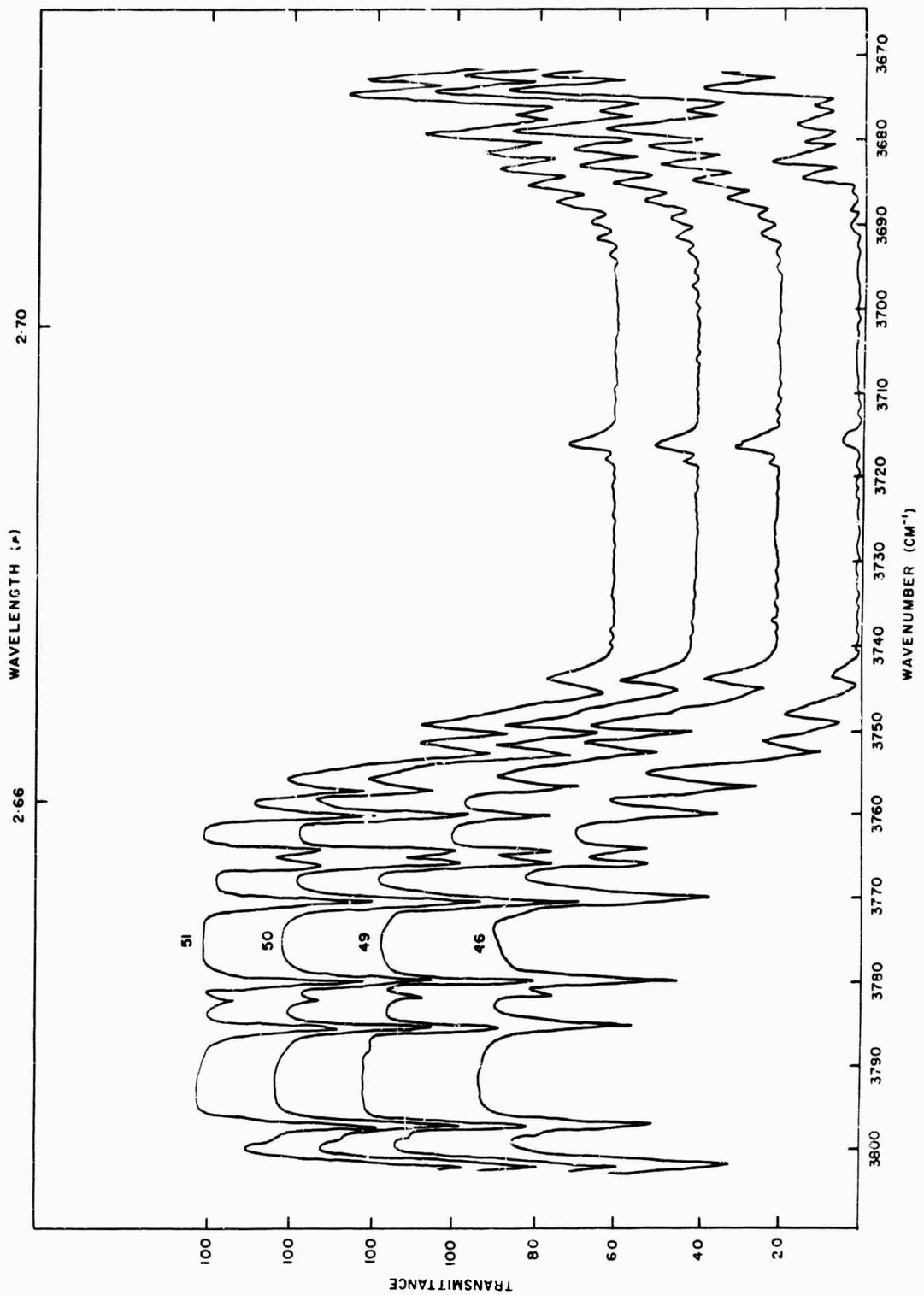
WAVELENGTH (μ)
2·66
2·70
WAVENUMBER (CM⁻¹)
3800
3790
3780
3770
3760
3750
3740
3730
3720
3710
3700
3690
3680
3670
TRANSMITTANCE
100
100
100
80
60
40
20
51
50
49
46

Figure 7

Aimospheric transmittance versus wave-number as observed at various altitudes for the region 3690-3560 cm^{-1}.

Fairbanks, Alaska July 13, 1964

Rec.	Time (AST)	h (km)	P (mb)	Zenith ∢
46	2133	19.2	62.7	89.74
49	2142	20.6	50.6	90.24
50	2145	21.0	47.7	90.40
51	2148	21.4	44.7	90.56

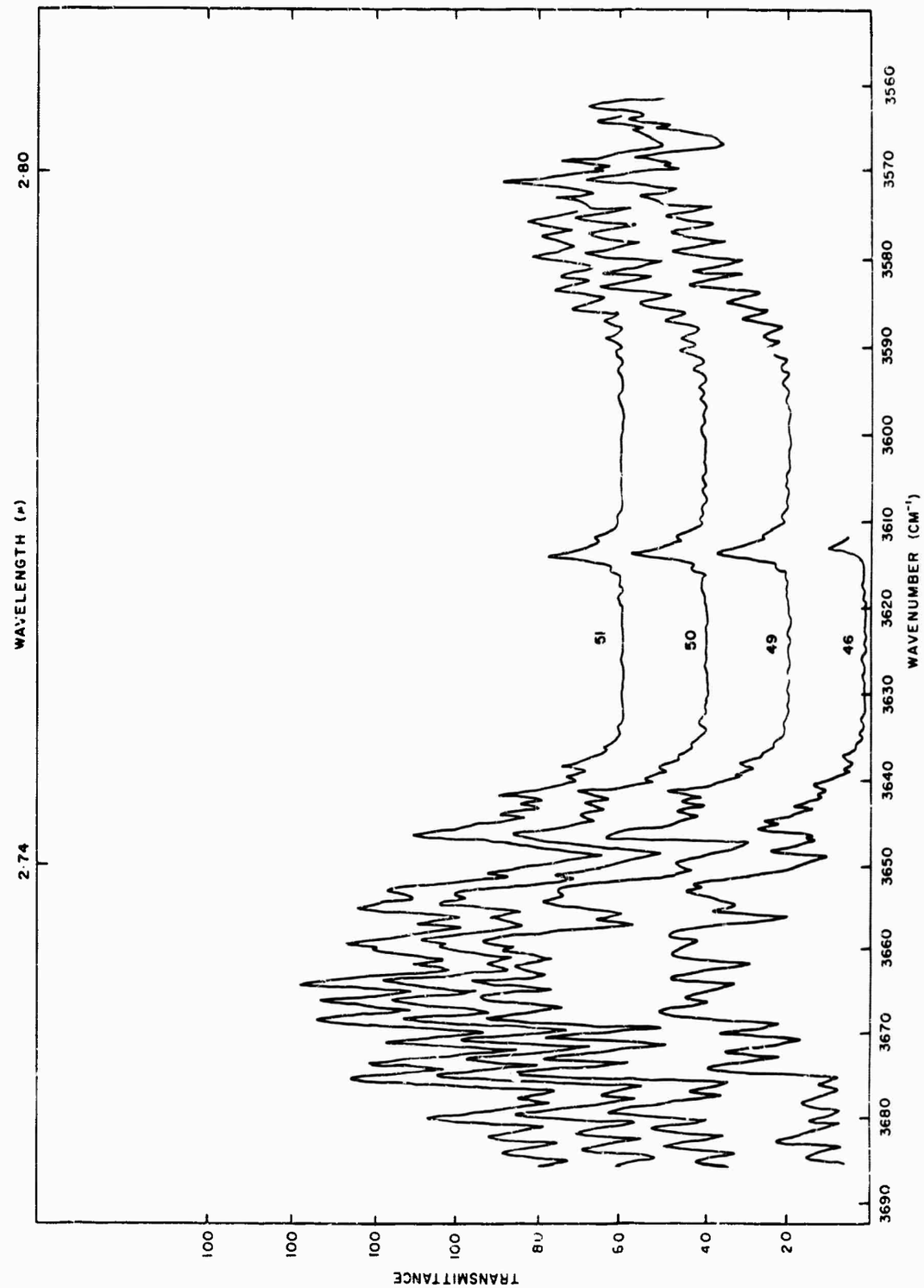
WAVELENGTH (μ)
2·74
2·80
WAVENUMBER (CM⁻¹)
3690
3680
3670
3660
3650
3640
3630
3620
3610
3600
3590
3580
3570
3560
TRANSMITTANCE
100
100
100
80
60
40
20
51
50
49
46

Figure 8

Atmospheric transmittance versus wavenumber as observed at various altitudes for the region 3920-3790 cm^{-1}.

Fairbanks, Alaska July 1[illegible], 1964

Rec.	Time (AST)	h (km)	P (mb)	Zenith ∢
54	2157	22.6	37.0	91.02
57	2207	23.5	32.3	91.44
58	2210	3.8	30.8	91.55
68	2240	26.7	19.6	92.70
70	2246	27.2	18.0	92.91

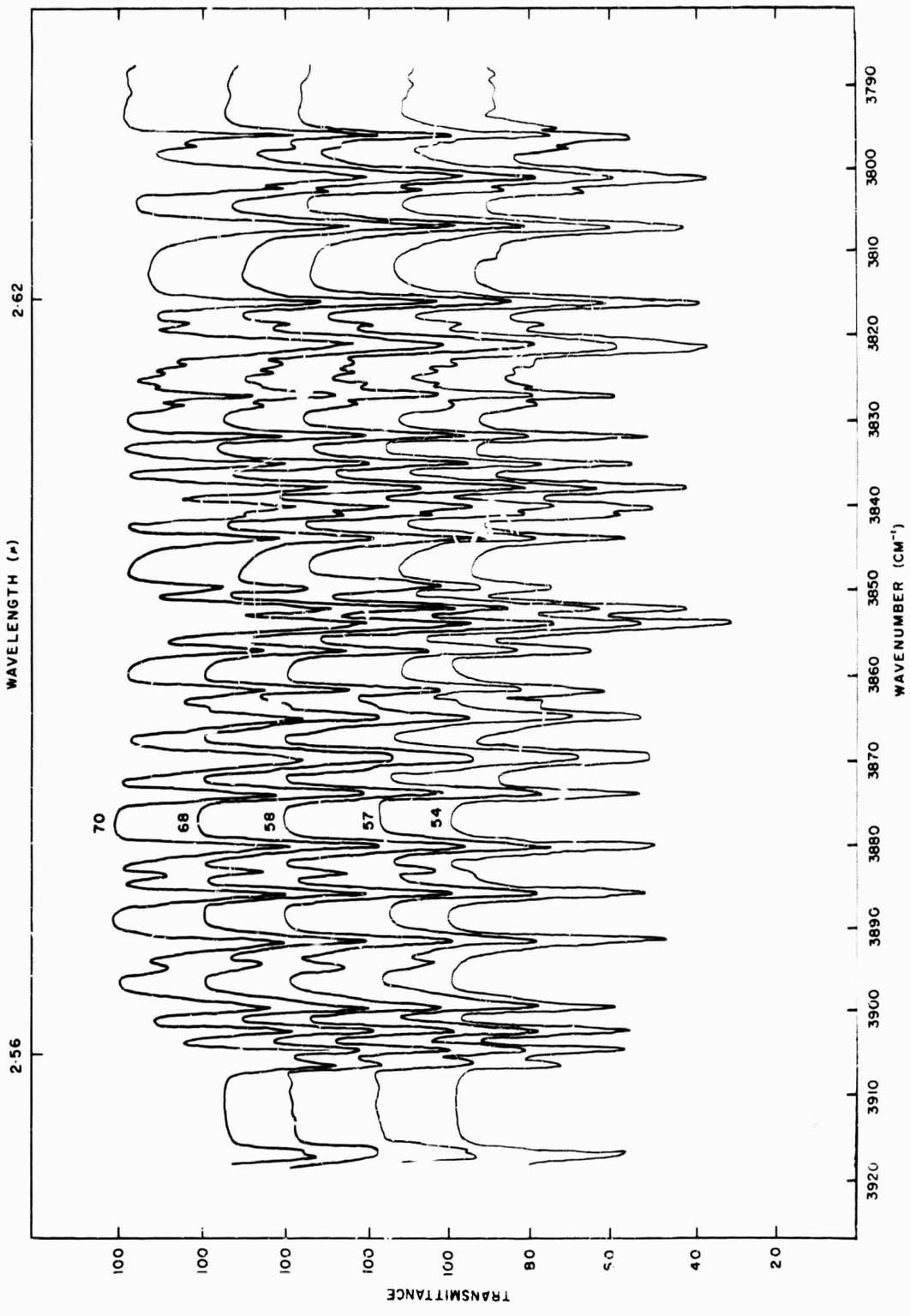
WAVELENGTH (μ)
2·56
2·62
WAVENUMBER (CM⁻¹)
3790
3800
3810
3820
3830
3840
3850
3860
3870
3880
3890
3900
3910
3920
TRANSMITTANCE
100
100
100
100
100
80
60
40
20
70
68
58
57
54

Figure 9

Atmospheric transmittance versus wave-number as observed at various altitudes for the region 3890-3670 cm^{-1}.

Fairbanks, Alaska July 13, 1964

Rec.	Time (AST)	h (km)	I (mb)	Zenith ∢
54	2157	22.6	37.0	91.02
57	2207	23.5	32.3	91.44
58	2210	23.8	30.8	91.55
68	2240	26.7	19.6	92.70
70	2246	27.2	18.0	92.91

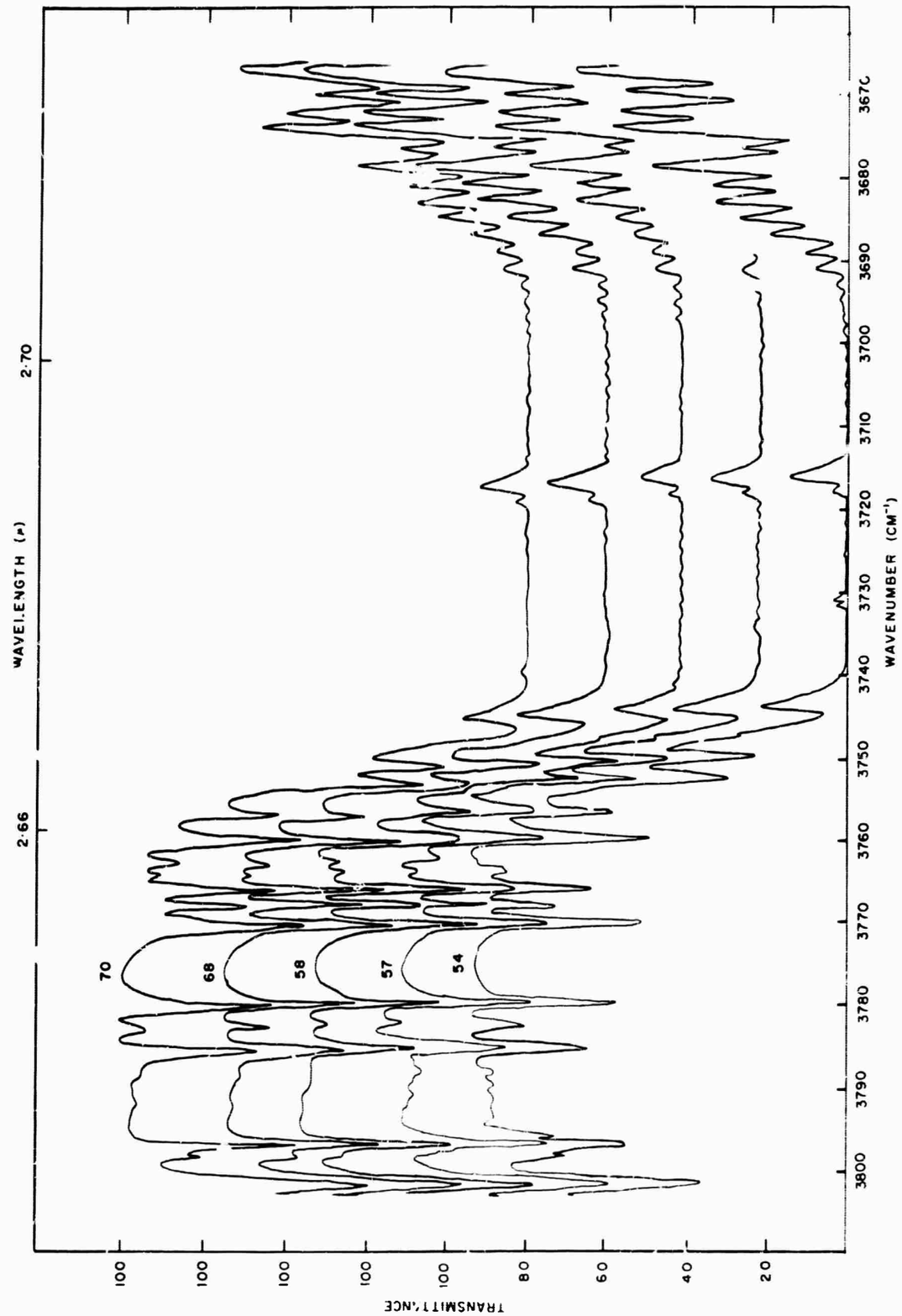
WAVELENGTH (μ)
2·66
2·70
WAVENUMBER (CM⁻¹)
3800
3790
3780
3770
3760
3750
3740
3730
3720
3710
3700
3690
3680
TRANSMITTANCE
100
100
100
100
80
60
40
20
70
68
58
57
54

Figure 10

Atmospheric transmittance versus wave-number as observed at various altitudes for the region 3680-3540 cm^{-1}.

Fairbanks, Alaska July 13, 1964

Rec.	Time (AST)	h (km)	P (mb)	Zenith ∢
54	2157	22.6	37.0	91.02
57	2207	23.5	32.3	91.44
58	2210	23.8	30.8	91.55
68	2240	26.7	19.6	92.70
70	2246	27.?	18.0	92.91

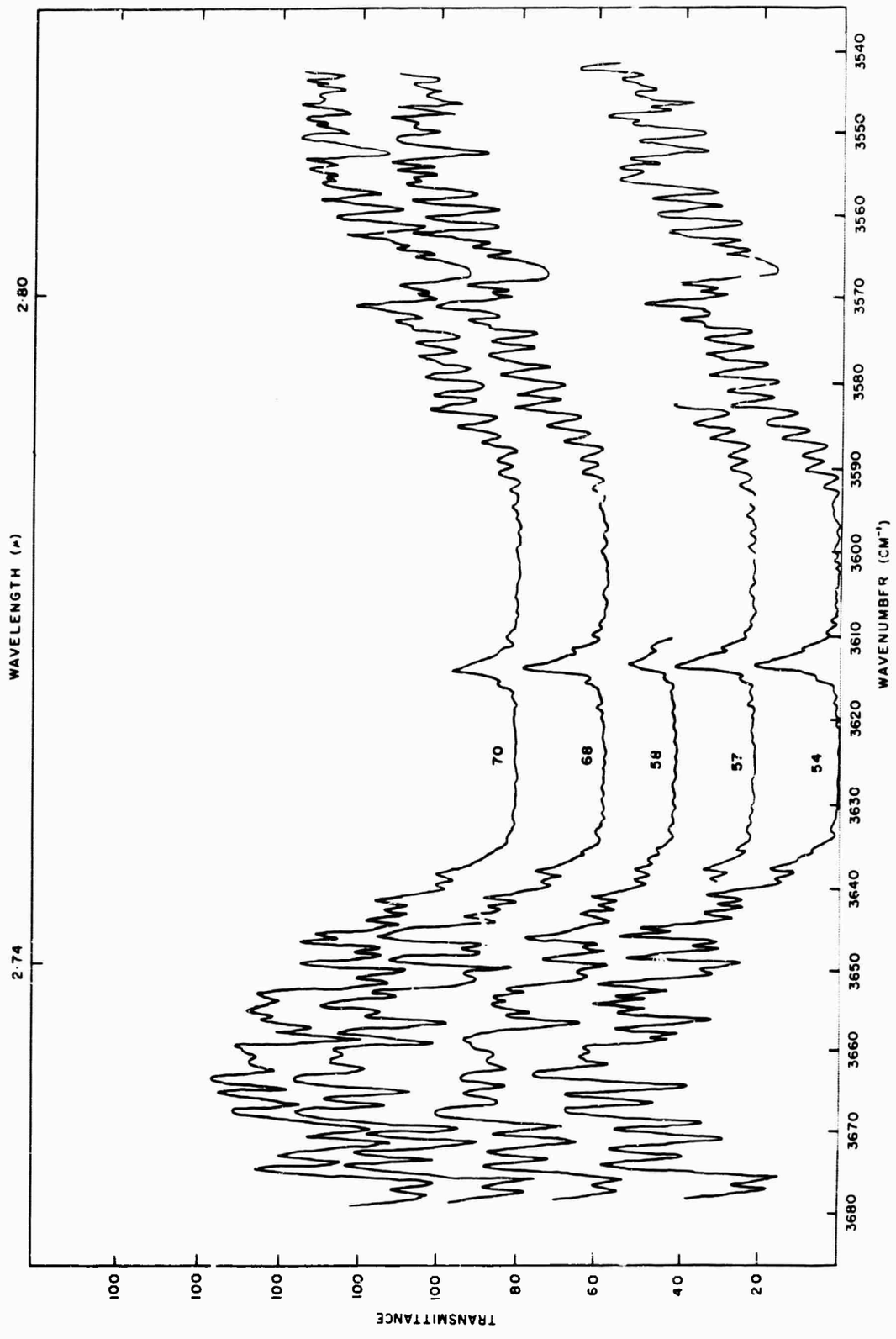
WAVELENGTH (μ)
2·74
2·80
WAVENUMBER (CM⁻¹)
3680
3670
3660
3650
3640
3630
3620
3610
3600
3590
3580
3570
3560
3550
3540
TRANSMITTANCE
100
100
100
100
80
60
40
20
70
68
58
57
54

Figure 11

Atmospheric transmittance versus wavenumber as observed at various altitudes for the region 3920-3790 cm^{-1}.

Fairbanks, Alaska July 21, 1964

Rec.	Time (AST)	h (km)	P (mb)	Zenith ∢
12	1420	7.18	400	50.37
13	1423	7.96	358	50.60
14	1426	8.73	320	50.83
15	1429	9.47	287	51.07
18	1438	11.2	220	51.80

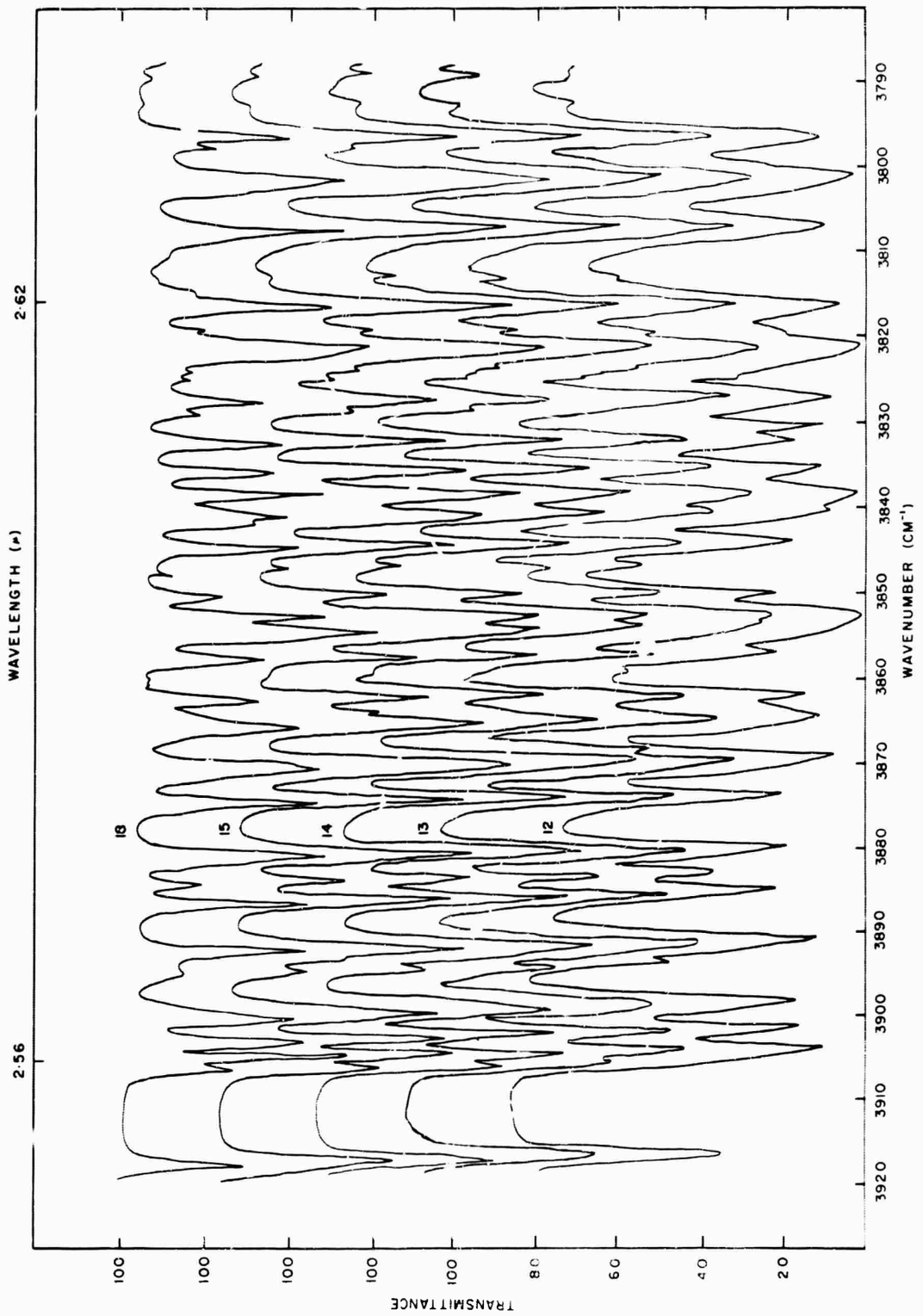
WAVELENGTH (μ)
2.56
2.62
WAVENUMBER (CM⁻¹)
3920
3910
3900
3890
3880
3870
3860
3850
3840
3830
3820
3810
3800
3790
TRANSMITTANCE
100
100
100
100
80
60
40
20
18
15
14
13
12

Figure 12

Atmospheric transmittance versus wave-number as observed at various altitudes for the region 3800-3670 cm^{-1}.

Fairbanks, Alaska July 21, 1964

Rec.	Time (AST)	h (km)	P (mb)	Zenith ∢
12	1420	7.18	400	50.37
13	1423	7.96	358	50.60
14	1426	8.73	320	50.83
15	1429	9.47	287	51.07
18	1438	11.2	220	51.80

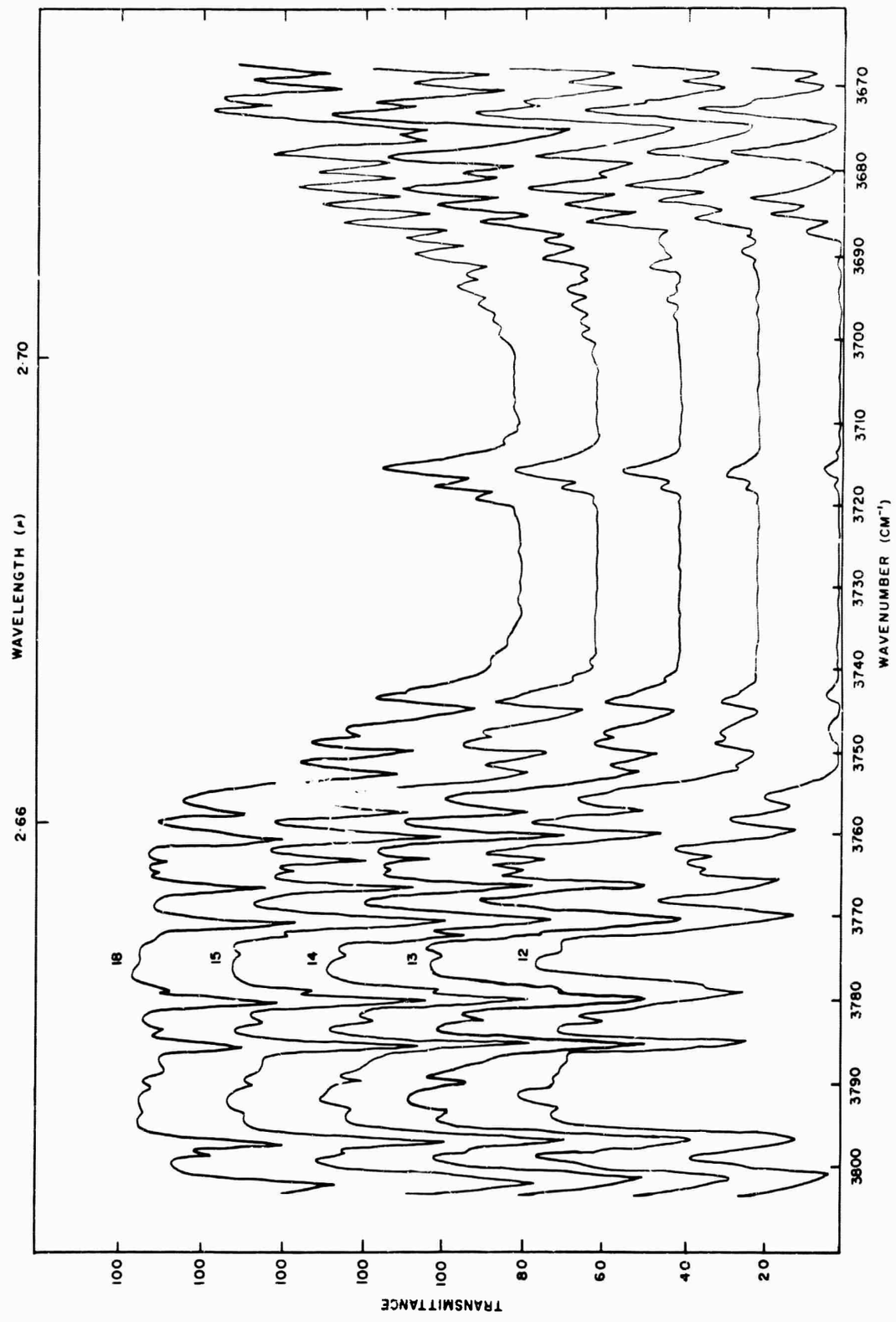
WAVELENGTH (μ)
2·66
2·70
WAVENUMBER (CM⁻¹)
3800
3790
3780
3770
3760
3750
3740
3730
3720
3710
3700
3690
3680
3670
TRANSMITTANCE
100
100
100
100
80
60
40
20
18
15
14
13
12

Figure 13

Atmospheric transmittance versus wavenumber as observed at various altitudes for the region 3680-3550 cm^{-1}.

Fairbanks, Alaska July 21, 1964

Rec.	Time (AST)	h (km)	P (mb)	Zenith ∢
12	1420	7.18	400	50.37
13	1423	7.96	358	50.60
14	1426	8.73	320	50.83
15	1429	9.47	287	51.07
18	1438	11.2	220	51.80

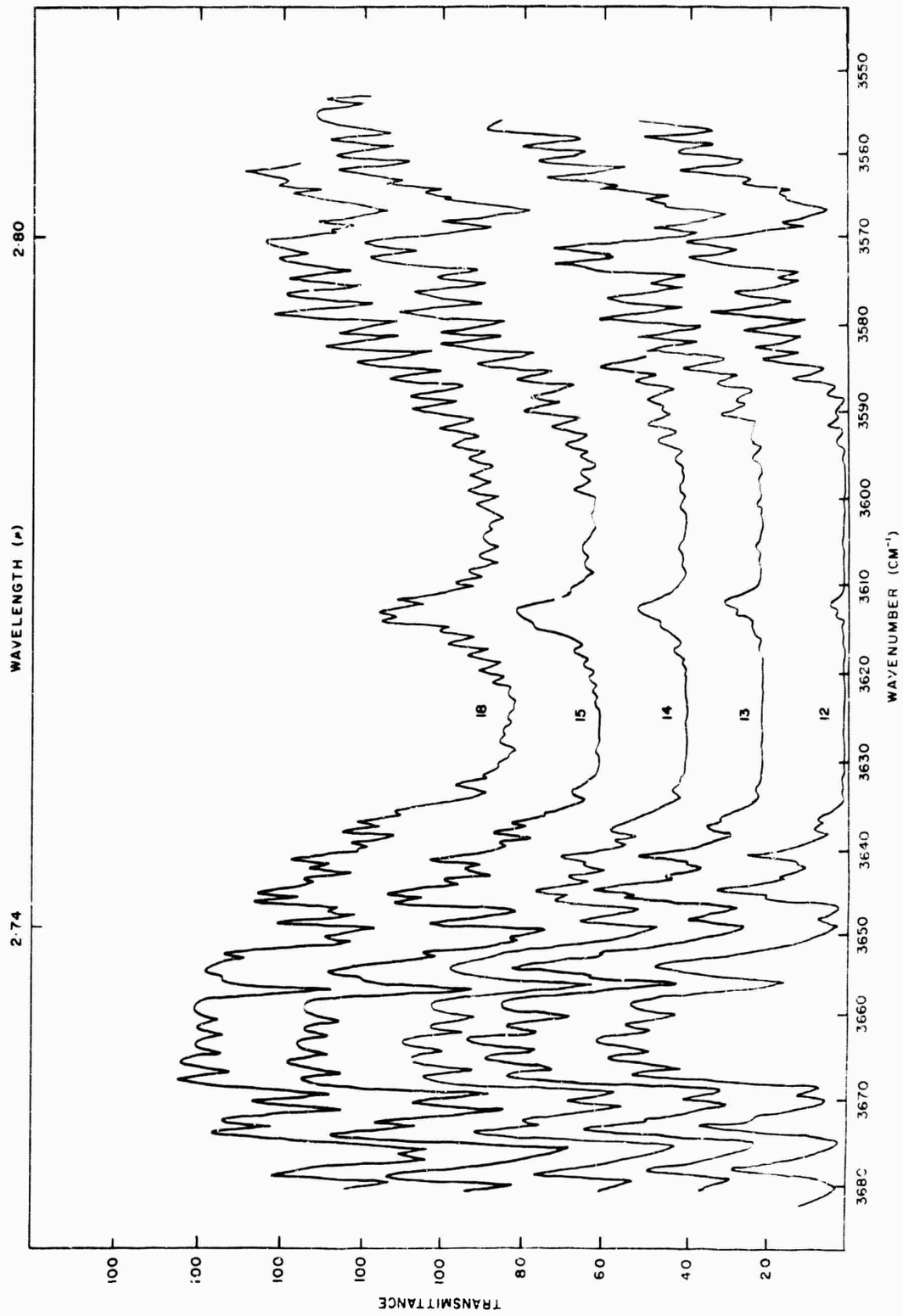
WAVELENGTH (μ)
2·74
2·80
WAVENUMBER (CM⁻¹)
3680
3670
3660
3650
3640
3630
3620
3610
3600
3590
3580
3570
3560
3550
TRANSMITTANCE
100
100
100
100
80
60
40
20
18
15
14
13
12

Figure 14

Atmospheric transmittance versus wave-number as observed at various altitudes for the region 3920-3790 cm^{-1}.

Fairbanks, Alaska July 21, 1964

Rec.	Time (AST)	h (km)	P (mb)	Zenith ∢
19	1441	11.7	205	52.05
21	1447	12.6	177	52.91
25	1459	14.5	131	53.70
28	1508	15.9	105	54.52

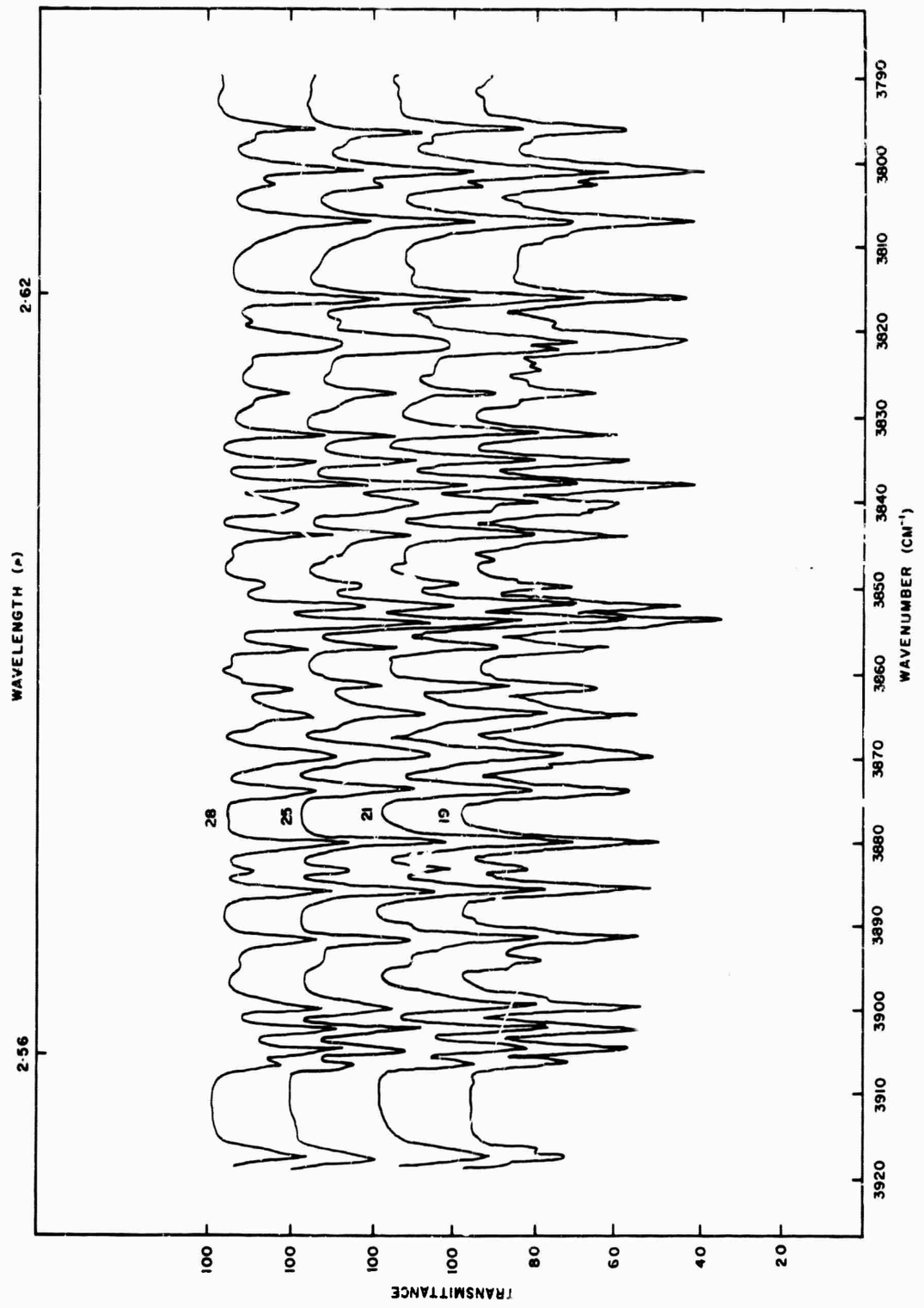
WAVELENGTH (μ)
2·56
2·62
WAVENUMBER (CM⁻¹)
3920
3910
3900
3890
3880
3870
3860
3850
3840
3830
3820
3810
3800
3790
TRANSMITTANCE
100
100
100
100
80
60
40
20
28
25
21
19

Figure 15

Atmospheric transmittance versus wavenumber as observed at various altitudes for the region 3800-3670 cm^{-1}.

Fairbanks, Alaska July 21, 1964

Rec.	Time (AST)	h (km)	P (mb)	Zenith ∢
19	1441	11.7	205	52.05
21	1447	12.6	177	52.91
25	1459	14.5	131	53.70
28	1508	15.9	105	54.52

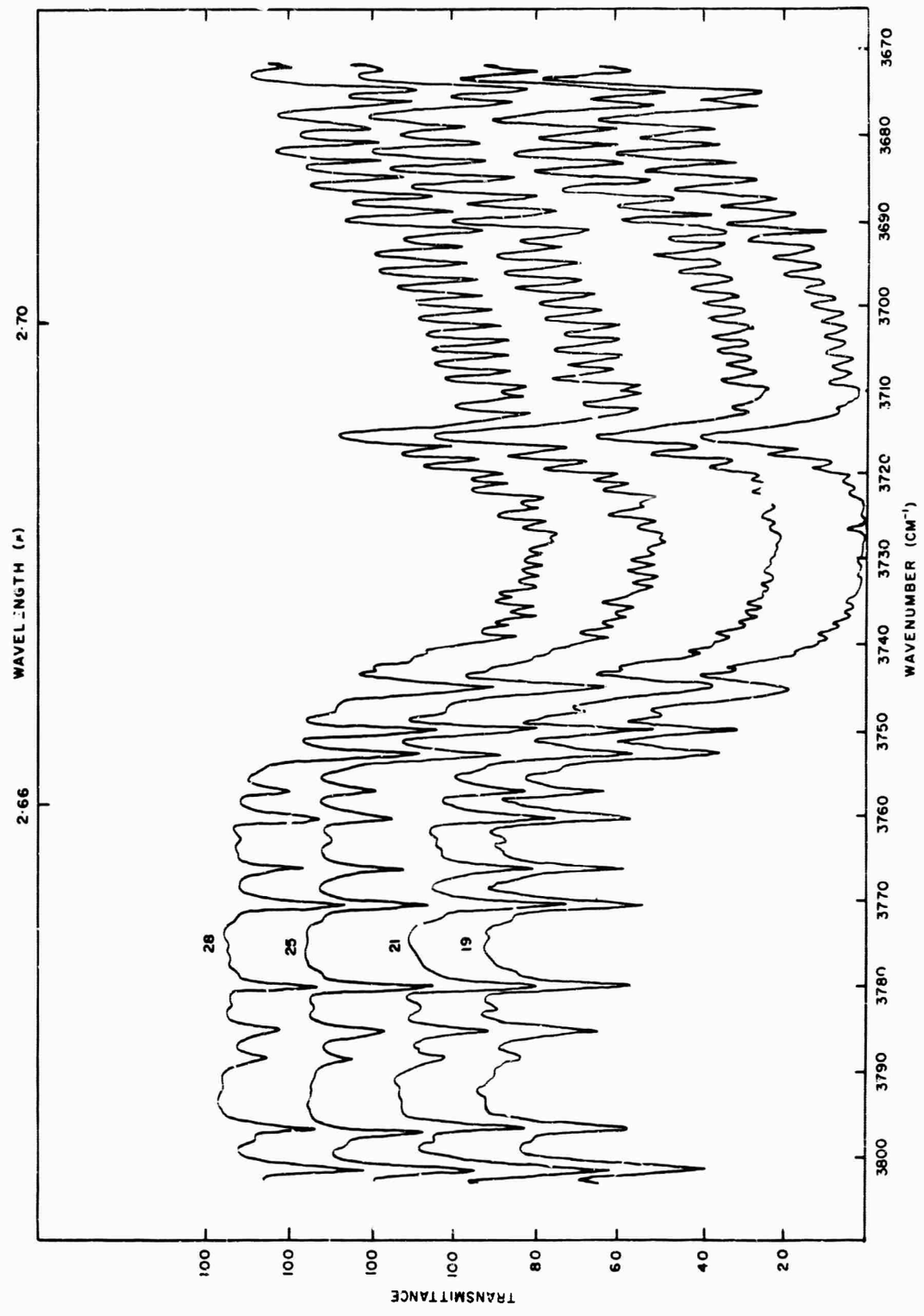
WAVELENGTH (μ)
2·66
2·70
WAVENUMBER (CM⁻¹)
3800
3790
3780
3770
3760
3750
3740
3730
3720
3710
3700
3690
3680
3670
TRANSMITTANCE
100
100
100
80
60
40
20
28
25
21
19

Figure 16

Atmospheric transmittance versus wavenumber as observed at various altitudes for the region 3690-3560 cm^{-1}.

Fairbanks, Alaska July 21, 1964

Rec.	Time (AST)	h (km)	P (mb)	Zenith ∢
19	1441	11.7	205	52.05
21	1447	12.6	177	52.91
25	1459	14.5	131	53.70
28	1508	15.9	105	54.52

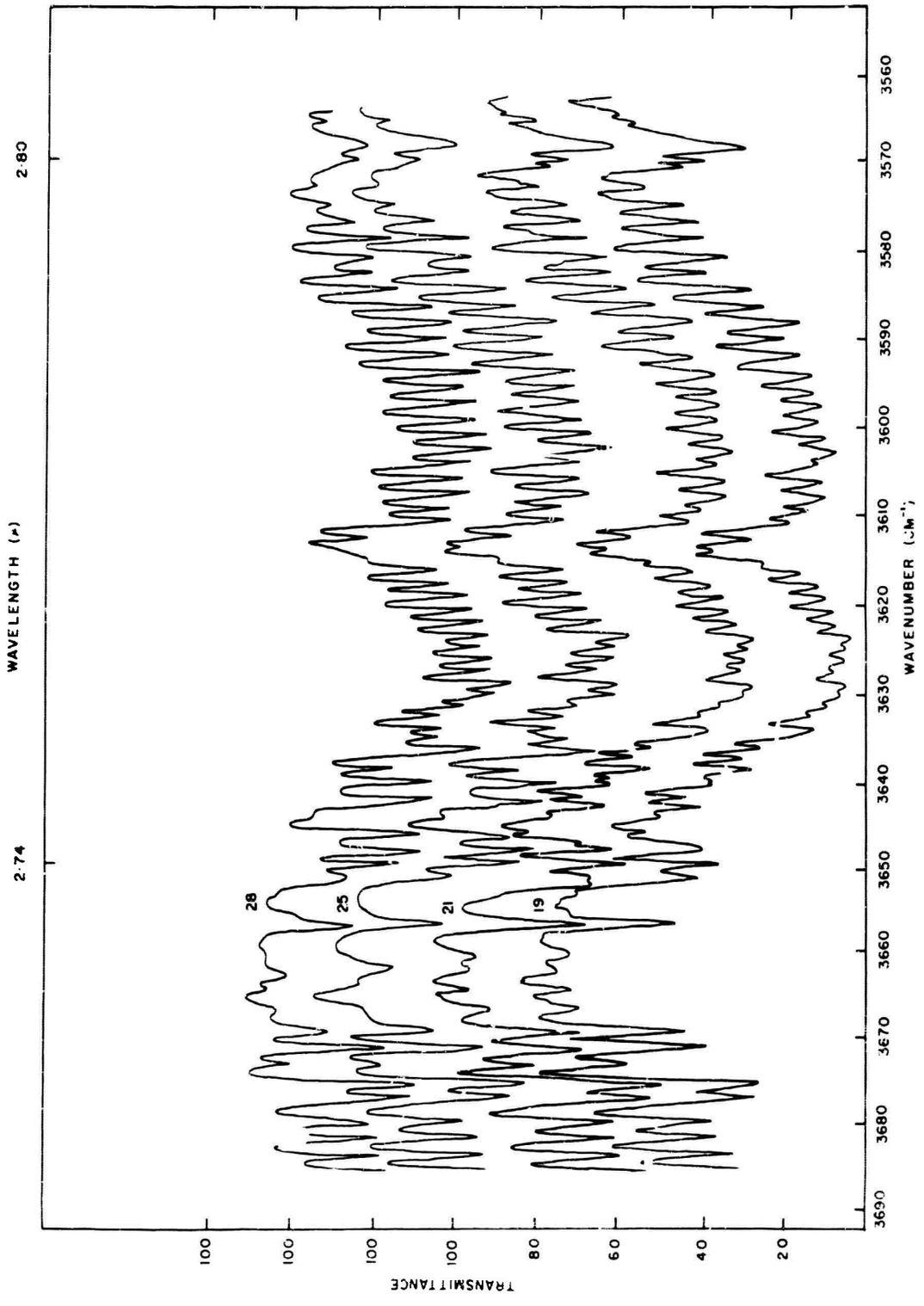
WAVELENGTH (μ)
2·74
2·80
WAVENUMBER (cm⁻¹)
3690
3680
3670
3660
3650
3640
3630
3620
3610
3600
3590
3580
3570
3560
TRANSMITTANCE
100
100
100
80
60
40
20
28
25
21
19

Figure 17

Atmospheric transmittance versus wavenumber as observed at various altitudes for the region 3920-3790 cm^{-1}.

Fairbanks, Alaska July 21, 1964

Rec.	Time (AST)	h (km)	P (mb)	Zenith χ
37	1535	20.5	51.3	57.17
38	1538	21.0	47.4	57.46
40	1544	22.1	40.1	58.06
43	1553	24.0	30.1	58.94

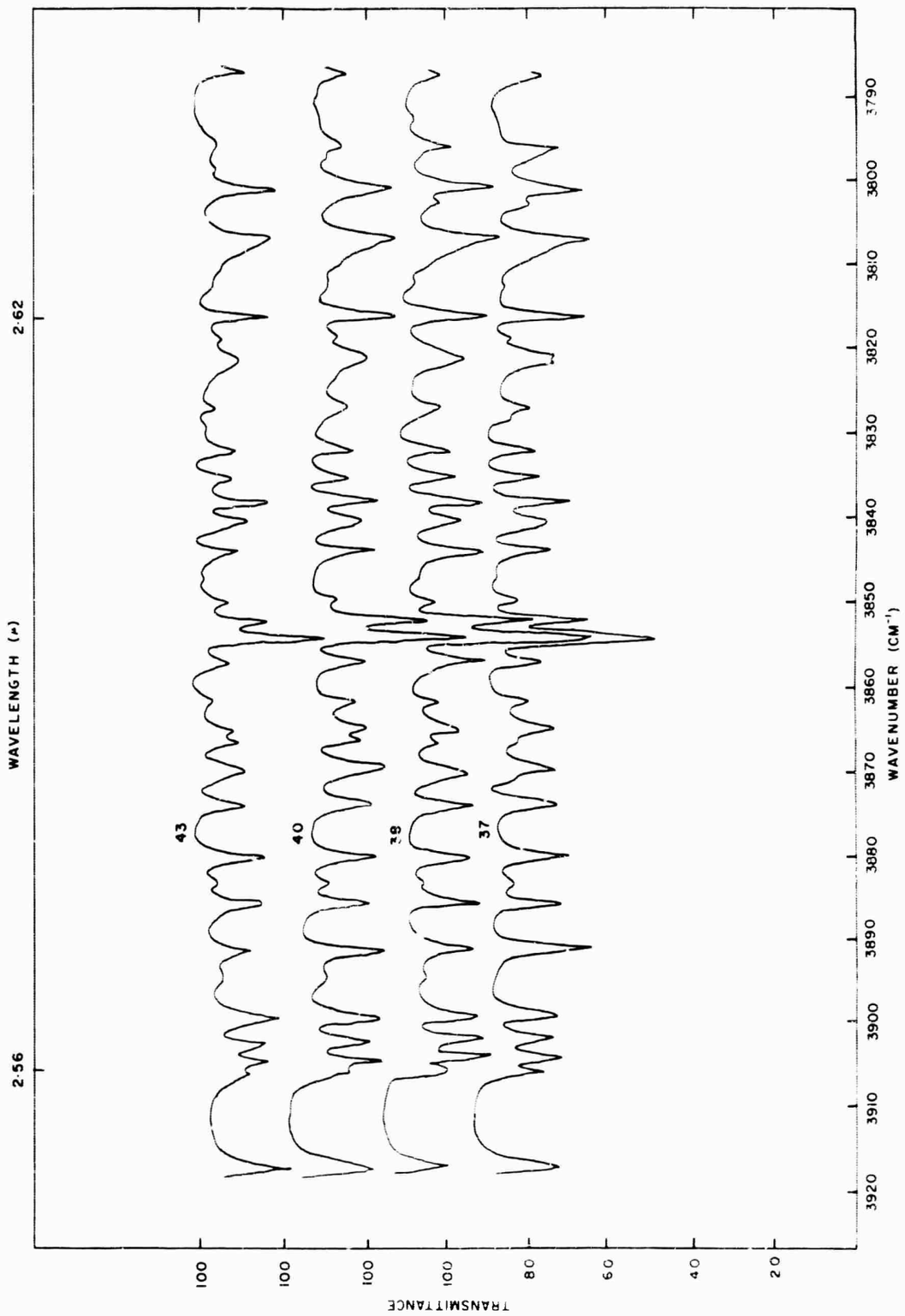
WAVELENGTH (μ)
2·56
2·62
WAVENUMBER (CM⁻¹)
3920
3910
3900
3890
3880
3870
3860
3850
3840
3830
3820
3810
3800
3790
TRANSMITTANCE
100
100
100
100
80
60
40
20
43
40
39
37

Figure 18

Atmospheric transmittance versus wavenumber as observed at various altitudes for the region 3800-3690 cm^{-1}.

Fairbanks, Alaska July 21, 1964

Rec.	Time (AST)	h (km)	P (mb)	Zenith ∢
37	1535	20.5	51.3	57.17
38	1538	21.0	47.4	57.46
40	1544	22.1	40.1	58.06
43	1553	24.0	30.1	58.94

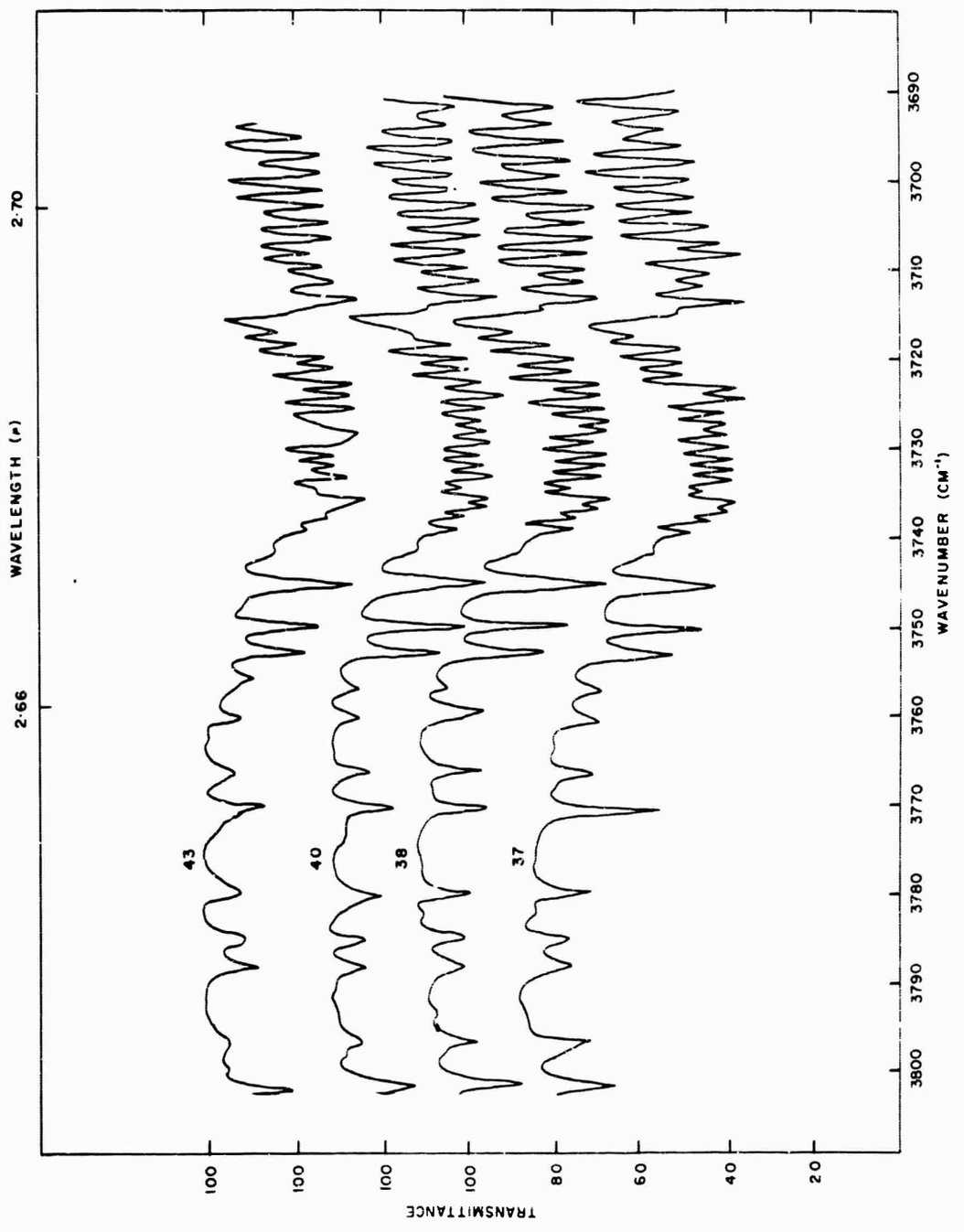
WAVELENGTH (μ)
2·66
2·70
WAVENUMBER (CM⁻¹)
3800
3790
3780
3770
3760
3750
3740
3730
3720
3710
3700
3690
TRANSMITTANCE
100
100
100
100
80
60
40
20
43
40
38
37

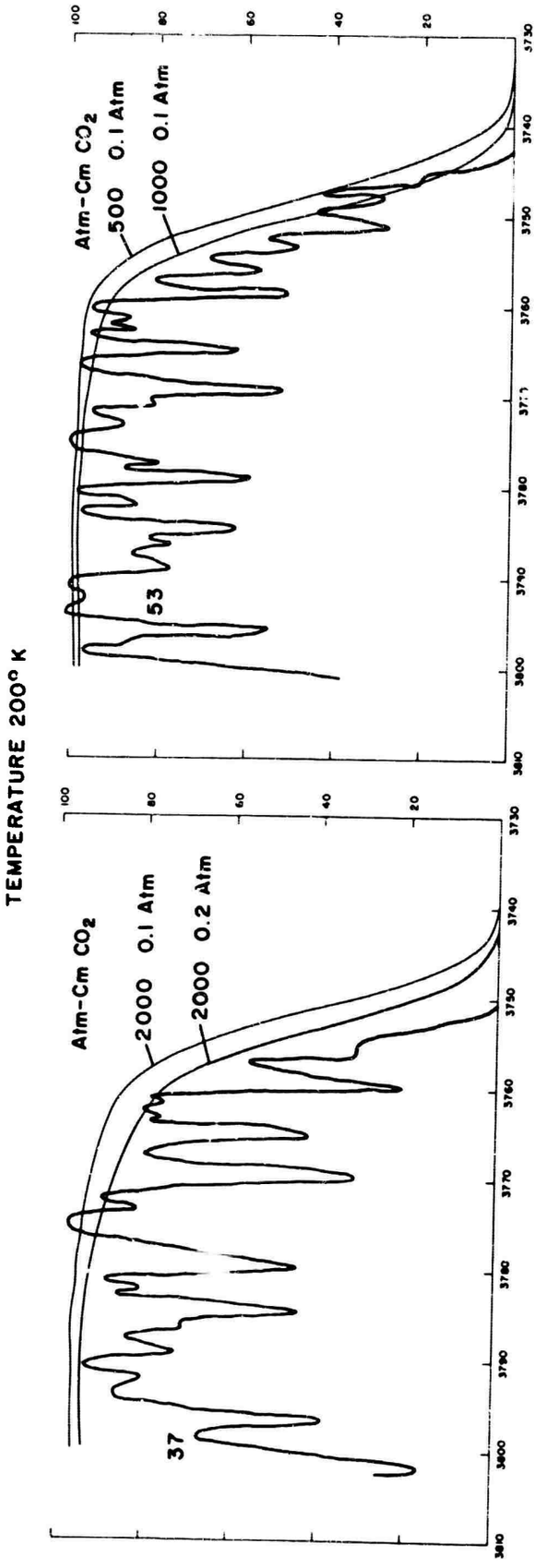

Figure 19

Figure 20

Comparison of the transmittance observed with the transmittance predicted by Plass[4] in the 3800 cm^{-1} to 3730 cm^{-1} region.

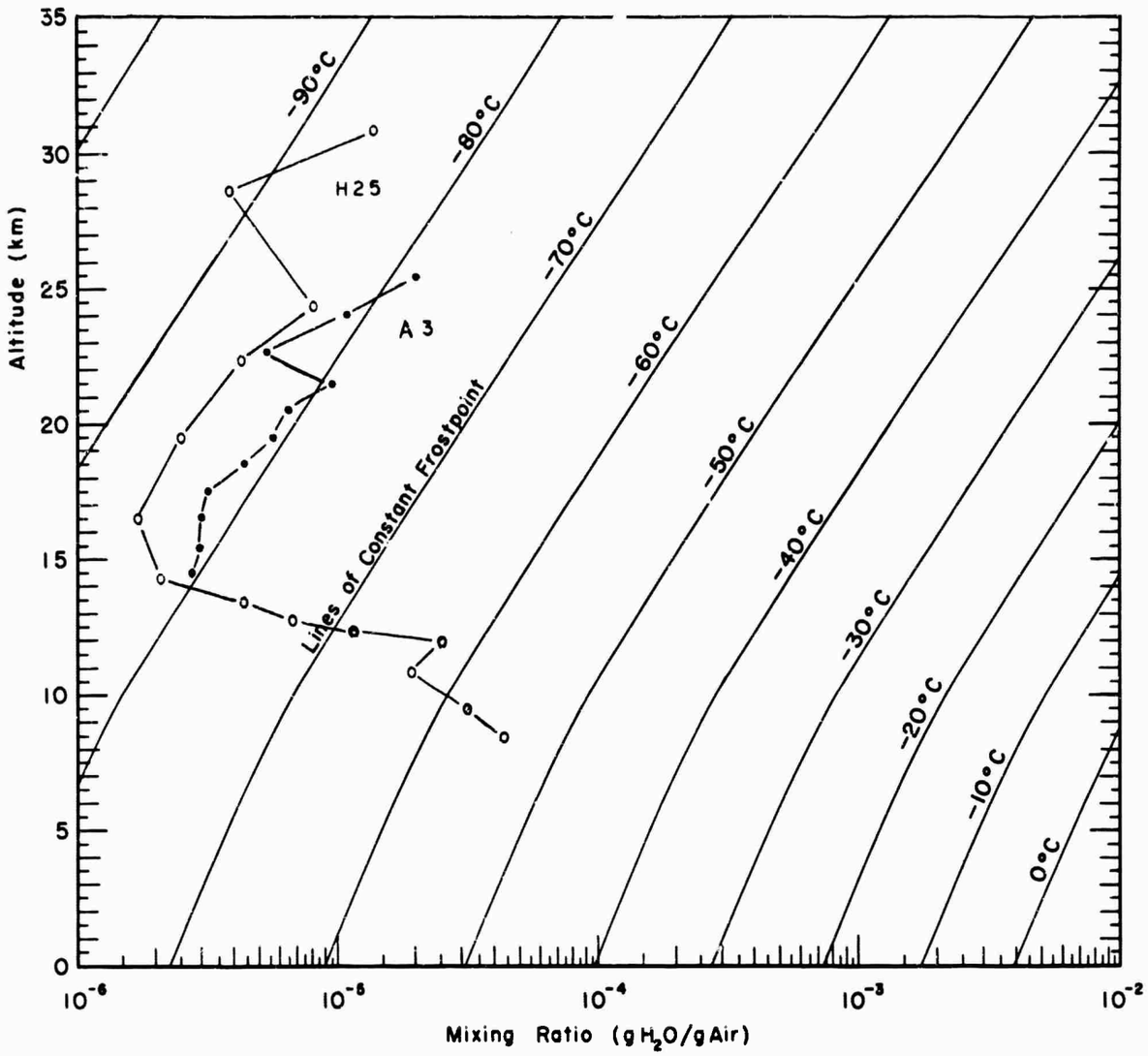

Figure 21. Water vapor mixing ratio profile as determined from the variation of the infrared absorption with altitude. The curve marked A-3 was determined from data obtained during the Alaskan flight. The curve marked H-25 was determined from data obtained during flight made from Holloman AFB, New Mexico.

TABLE I

Air Mass Traversed by Solar Radiation

Flight No.	Record No.	Air Mass kg/cm^2	Air Mass* kg/cm^2
A1	12	10.426	3.096
A1	23	9.931	5.989
A1	37	7.958	7.006
	53	3.072	2.689
	49	2.240	0.452
A2	50	2.283	0.700
A2	51	2.288	0.904
A2	54	2.420	1.469
A2	57	2.746	1.989
A2	58	2.856	2.192
A2	68	4.219	3.887
A2	70	4.845	4.497

*The air mass indicated in this column is that traversed by the radiation along the path from the balloon down to the minimum height H_0 and back up to the height of the balloon.

TABLE II

Mixing Ratio as Determined from Long Path Absorptions

Flight No.	Record No.	Av. Ht. km	Mixing Ratio g/g
A1	23	14.0	$4.8 \cdot 10^{-6}$
A1	37	16.3	$3.2 \cdot 10^{-6}$
A1	53	22.5	$4.4 \cdot 10^{-6}$
A2	54	22.6	$6.1 \cdot 10^{-6}$
A2	57	22.2	$4.8 \cdot 10^{-6}$
A2	58	22.2	$4.7 \cdot 10^{-6}$
A2	68	20.3	$3.0 \cdot 10^{-6}$

Unclassified
Security Classification

DOCUMENT CONTROL DATA - R&D
(Security classification of title, body of abstract and indexing annotation must be entered when the overall report is classified)

1. ORIGINATING ACTIVITY (Corporate author)	2a. REPORT SECURITY CLASSIFICATION
Department of Physics, University of Denver Denver, Coloardo 80210	Unclassified
	2b GROUP

3. REPORT TITLE

Atmospheric Absorptions Over Long Slant Paths in the Stratosphere

4. DESCRIPTIVE NOTES (Type of report and inclusive dates)

Scientific Report Interim

5. AUTHOR(S) (Last name, first name, initial)

Murcray, David G., Murcray, Frank H., Williams, Walter J.

6. REPORT DATE	7a. TOTAL NO. OF PAGES	7b. NO. OF REFS
October 1966	57	5

8a. CONTRACT OR GRANT NO.	9a. ORIGINATOR'S REPORT NUMBER(S)
AF 19(628)-5202 ARPA ORDER No. 363 b. PROJECT NO. 8662-01 c. 6250301R d. None	Scientific Report No. 4 9b. OTHER REPORT NO(S) (Any other numbers that may be assigned this report) AFCRL-66-812

10. AVAILABILITY/LIMITATION NOTICES

Distribution of this document is unlimited

11. SUPPLEMENTARY NOTES	12. SPONSORING MILITARY ACTIVITY
Hq. AFCRL, OAR (CRO) United States Air Force L.G. Hanscom Field, Bedford, Mass.	Advanced Research Projects Agency

13. ABSTRACT

The variation of the infrared solar spectrum with altitude was observed during a series of balloon flights made from Fairbanks, Alaska. Spectra were obtained at various altitudes with solar zenith angles ranging from 49° to 92°. These spectra were used to determine the atmospheric transmittance to be expected at high altitudes and particularly over very long slant paths in the stratosphere. The transmittance data are presented in this report.

The spectral region scanned during this flight covered the 2.7 μ region. The major atmospheric absorptions in this region are due to carbon dioxide and water vapor. The paths traversed by the solar radiation in reaching the spectrometer when the solar zenith angle is greater than 90° are such that a major portion of the air mass traversed by the radiation is traversed in a relatively narrow altitude interval close to the minimum height of the ray. Thus these long paths provide a method of sampling the absorption to be expected in relatively narrow layers. The water vapor absorptions obtained under these conditions have been used to determine the amount of water vapor present in these layers in the stratosphere. These data are compared with the mixing ratios determined on the basis of the change in these absorptions during a flight with small solar zenith angle. The agreement is within the accuracy of the measurement and shows no indication that the data of the normal flight are inaccurate due to contamination. The profile indicates the increased mixing ratio above the tropopause noted on other flights at other geographic locations.

DD FORM 1 JAN 64 1473

Unclassified
Security Classification

14. KEY WORDS	LINK A		LINK B		LINK C	
	ROLE	WT	ROLE	WT	ROLE	WT
Solar Spectrum						
Infrared Spectrum						
Telluric Transmittance						
Stratospheric Water Vapor						

INSTRUCTIONS

1. ORIGINATING ACTIVITY: Enter the name and address of the contractor, subcontractor, grantee, Department of Defense activity or other organization *(corporate author)* issuing the report.

2*a*. REPORT SECURITY CLASSIFICATION: Enter the overall security classification of the report. Indicate whether "Restricted Data" is included. Marking is to be in accordance with appropriate security regulations.

2*b*. GROUP: Automatic downgrading is specified in DoD Directive 5200.10 and Armed Forces Industrial Manual. Enter the group number. Also, when applicable show that optional markings have been used for Group 3 and Group 4 as authorized.

3. REPORT TITLE: Enter the complete report title in all capital letters. Titles in all cases should be unclassified. If a meaningful title cannot be selected without classification, show title classification in all capitals in parenthesis immediately following the title.

4. DESCRIPTIVE NOTES: If appropriate, enter the type of report, e.g., interim, progress, summary, annual, or final. Give the inclusive dates when a specific reporting period is covered.

5. AUTHOR(S): Enter the name(s) of author(s) as shown on or in the report. Enter last name, first name, middle initial. If military, show rank and branch of service. The name of the principal author is an absolute minimum requirement.

6. REPORT DATE: Enter the date of the report as day, month, year; or month, year. If more than one date appears on the report, use date of publication.

7*a*. TOTAL NUMBER OF PAGES: The total page count should follow normal pagination procedures, i.e., enter the number of pages containing information.

7*b*. NUMBER OF REFERENCES: Enter the total number of references cited in the report.

8*a*. CONTRACT OR GRANT NUMBER: If appropriate, enter the applicable number of the contract or grant under which the report was written.

8*b*, 8*c*, & 8*d*. PROJECT NUMBER: Enter the appropriate military department identification, such as project number, subproject number, system numbers, task number, etc.

9*a*. ORIGINATOR'S REPORT NUMBER(S): Enter the official report number by which the document will be identified and controlled by the originating activity. This number must be unique to this report.

9*b*. OTHER REPORT NUMBER(S): If the report has been assigned any other report numbers *(either by the originator or by the sponsor)*, also enter this number(s).

10. AVAILABILITY/LIMITATION NOTICES: Enter any limitations on further dissemination of the report, other than those imposed by security classification, using standard statements such as:

(1) "Qualified requesters may obtain copies of this report from DDC."

(2) "Foreign announcement and dissemination of this report by DDC is not authorized."

(3) "U. S. Government agencies may obtain copies of this report directly from DDC. Other qualified DDC users shall request through _____."

(4) "U. S. military agencies may obtain copies of this report directly from DDC. Other qualified users shall request through _____."

(5) "All distribution of this report is controlled. Qualified DDC users shall request through _____."

If the report has been furnished to the Office of Technical Services, Department of Commerce, for sale to the public, indicate this fact and enter the price, if known.

11. SUPPLEMENTARY NOTES: Use for additional explanatory notes.

12. SPONSORING MILITARY ACTIVITY: Enter the name of the departmental project office or laboratory sponsoring *(paying for)* the research and development. Include address.

13. ABSTRACT: Enter an abstract giving a brief and factual summary of the document indicative of the report, even though it may also appear elsewhere in the body of the technical report. If additional space is required, a continuation sheet shall be attached.

It is highly desirable that the abstract of classified reports be unclassified. Each paragraph of the abstract shall end with an indication of the military security classification of the information in the paragraph, represented as *(TS)*, *(S)*, *(C)*, or *(U)*.

There is no limitation on the length of the abstract. However, the suggested length is from 150 to 225 words.

14. KEY WORDS: Key words are technically meaningful terms or short phrases that characterize a report and may be used as index entries for cataloging the report. Key words must be selected so that no security classification is required. Identifiers, such as equipment model designation, trade name, military project code name, geographic location, may be used as key words but will be followed by an indication of technical context. The assignment of links, rules, and weights is optional.